Experimental Demonstration of Photovoltaic Powered Solar Cooling With Ice Storage

by

Tobin Peyton-Levine

A Thesis Presented in Partial Fulfillment
of the Requirements for the Degree
Master of Science

Approved June 2012 by the
Graduate Supervisory Committee:

Dr. Patrick Phelan, Chair
Dr. Steven Trimble
Dr. Robert Wang

ARIZONA STATE UNIVERSITY

August 2012

ABSTRACT

The ability to shift the photovoltaic (PV) power curve and make the energy accessible during peak hours can be accomplished through pairing solar PV with energy storage technologies. A prototype hybrid air conditioning system (HACS), built under supervision of project head Patrick Phelan, consists of PV modules running a DC compressor that operates a conventional HVAC system paired with a second evaporator submerged within a thermal storage tank. The thermal storage is a $0.284m^3$ or 75 gallon freezer filled with Cryogel balls, submerged in a weak glycol solution. It is paired with its own separate air handler, circulating the glycol solution. The refrigerant flow is controlled by solenoid valves that are electrically connected to a high and low temperature thermostat. During daylight hours, the PV modules run the DC compressor. The refrigerant flow is directed to the conventional HVAC air handler when cooling is needed. Once the desired room temperature is met, refrigerant flow is diverted to the thermal storage, storing excess PV power. During peak energy demand hours, the system uses only small amounts of grid power to pump the glycol solution through the air handler (note the compressor is off), allowing for money and energy savings. The conventional HVAC unit can be scaled down, since during times of large cooling demands the glycol air handler can be operated in parallel with the conventional HVAC unit.

Four major test scenarios were drawn up in order to fully comprehend the performance characteristics of the HACS. Upon initial running of the system, ice was produced and the thermal storage was charged. A simple test run consisting of discharging the thermal storage, initially ~¼ frozen, was performed. The glycol air handler ran for 6 hours and the initial cooling power was 4.5 kW. This initial test was significant, since greater than 3.5 kW of cooling power was produced for 3 hours, thus demonstrating the concept of energy storage and recovery.

DEDICATION

This thesis is dedicated to my parents, Bettina Peyton and Matthew Levine. They are the ones who have supported my decisions throughout my entire life and academic career. Thank you, Mom and Dad.

ACKNOWLEDGMENTS

This research was carried out with support from many members of the University community. Grateful acknowledgment is directed toward my primary advisor, Dr. Patrick Phelan, for noticing my talents and inviting me to be a part of his research team. Generous thanks to Jonathan Sherbeck for the amazing amount of help, insight, and knowledge that he provided throughout this whole process. Also to Dr. Steven Trimble and Dr. Robert Wang for being part of my review committee and providing thoughtful instruction. Finally, much thanks to mechanical and aerospace engineering lab manager, Bruce Steele, for his aid in troubleshooting data collection.

TABLE OF CONTENTS

LIST OF TABLES

Table Page

LIST OF FIGURES

Figure Page

Figure Page

NOMENCLATURE

A	Ampere
B_x	Bias uncertainty
C	Coulomb
C_p	Specific heat at constant pressure [J kg^{-1} K^{-1}]
COP	Coefficient of performance cooling
d	Diameter of a pipe [m]
DOE	Design of experiments
GPM	Gallons per minute
Q	Heating or Cooling load [kW_{th}]
HACS	Hybrid air conditioning system
HVAC	Heating ventilation and air conditioning
$\dot{m}$	Mass flow rate [kg s^{-1}]
n	Sample size
P_x	Precision uncertainty
Q_C	Heat removed from cold reservoir [W]
Q_{in}	Heat transfer rate [W]
RPM	Revolutions per minute
t	t-statistic
ΔT	Finite increment in temperature [K, ^oC]
U_x	Total uncertainty
$\dot{V}$	Volumetric flow rate [m^3 s^{-1}]
ρ	Density [kg m^{-3}]
Ω	Ohm [m^2 kg s^{-1} C^1]

PREFACE

The research presented in this paper is a culmination of the work of multiple students and professionals. The construction of the prototype system had been nearly completed by Jon Sherbeck and Nate Sanford before I joined the research team in August 2011. At that time, the prototype system consisted of the direct current "DC" compressor installed and in line with the two evaporators (conventional HVAC air handler and evaporator within the freezer for thermal storage). Installations to complete the prototype system included filling the thermal storage with Cryogel balls and a weak glycol solution, connecting the glycol pump and air handler, installing the PV modules, and creating the electrical device that differentiated between which source (Grid or PV) powered the system [1]. My role within the project consisted of finishing construction of the prototype system, installing all data acquisition devices, creating a program to log the data collected, creating an experimental design in order to test the abilities of the prototype system, and formulating a general coefficient of performance (COP) equation that can be used to compare the COP of the prototype to conventional HVAC units.

Chapter 1: INTRODUCTION

Extensive research on heating ventilating and air conditioning (HVAC) systems has been performed, aiming towards decreasing the energy needs and requirements of these systems. Theoretical models and numerical ratings, such as the coefficient of performance (COP) and cooling power have been developed in order to rate the efficiency of HVAC systems. The COP is the measure of the efficiency with which a heat pump operates. It directly correlates to the ability of the heat pump to either add heat to the hot reservoir (for heating) or remove heat from the interior (for cooling) [2]. The cooling power is a measure of the cooling load that the HVAC system can produce [3].

The Department of Defense sent out a proposal asking researchers to find ways to improve energy efficiency in buildings [4]. Dr. Patrick Phelan and John Sherbeck proposed a novel system, titled the Hybrid Air Conditioning System or HACS, in which a HVAC unit is powered by photovoltaic (PV) modules paired with ice thermal storage. This system is unique because it combines a direct current (DC) compressor with the PV modules in order to avoid electrical losses through an inverter. Along with the innovative idea of having a DC compressor, a second evaporator placed inside the ice thermal storage allows for the excess PV power to be stored and discharged for cooling during later hours. A complete prototype system was constructed along with an economic model

performed by a former student Sadiq Jubran [5]. Figure(1.1) shows the general timeline of the project until May 2012.

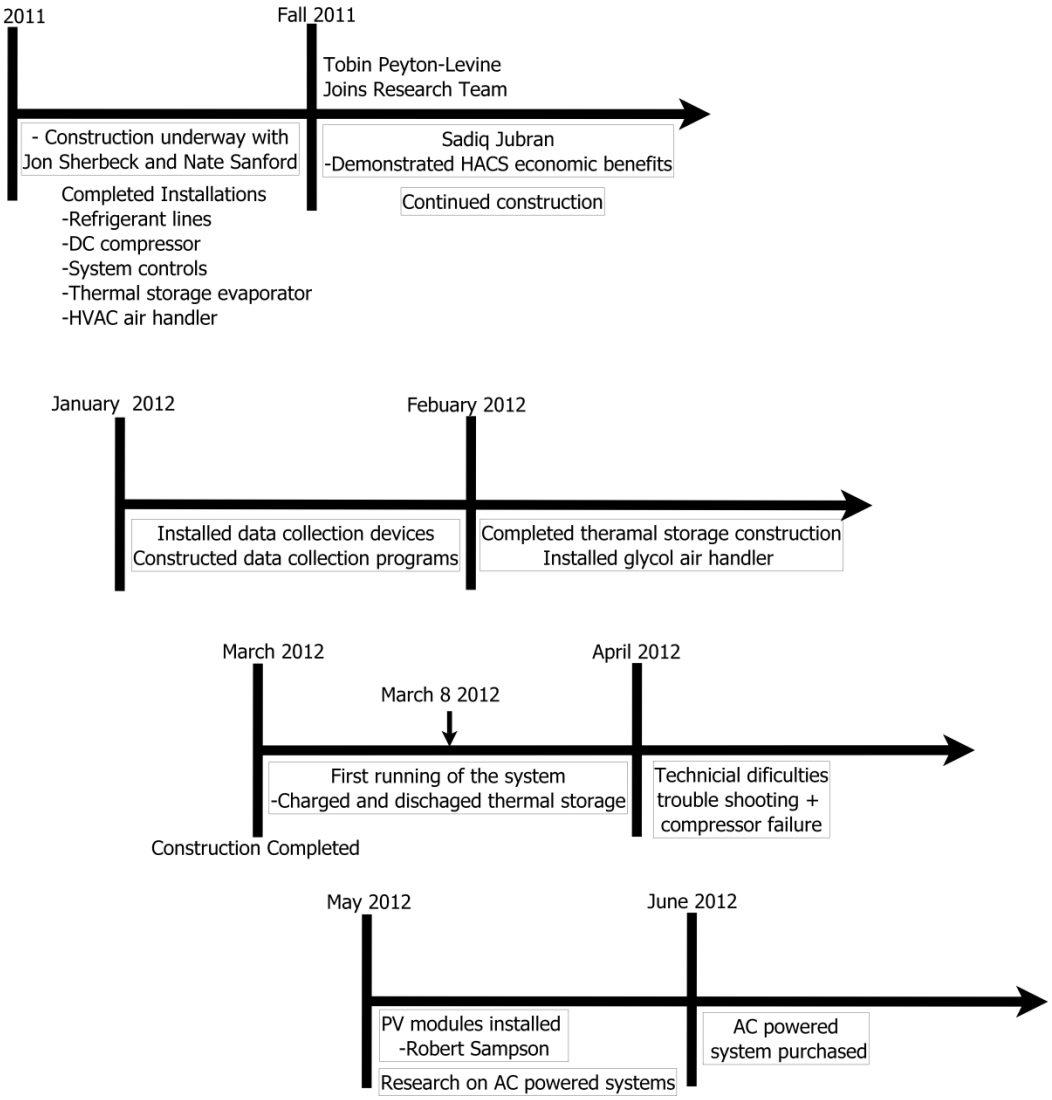

Figure 1.1 Project timeline

Looking at the timeline outlined in Fig(1.1), it is clear that the project has been in progress for almost two years. It is important to note the incident of compressor failure in May 2012. Due to the compressor failure, the abilities of the original HACS prototype could not be fully observed. Only one test, consisting of discharging the thermal storage,

could be performed. It should be noted that from this point forward, the discussion outlines the work performed by myself which includes comparisons between competing models, design of experiments for the original prototype system, an error analysis, data analysis and description, followed by the research and concurrent move towards building an AC powered system. Ultimately, despite the minimal amount of run time and data collected, the prototype system fully demonstrated that energy can be stored and accessed during later hours to provide cooling.

1:1 MOTIVATION

This prototype hybrid air conditioning system (HACS) was originally built for use in forward operating bases (FOB's) in order to help decrease their energy requirements. Reducing a FOB's energy needs leads to a decrease in the size of the resupply transports, and most importantly, fewer lives need be put at risk. For this reason, the prototype system was designed to be easily transported and installed.

Recently it has been noted that the HACS can be used for residential and commercial purposes also. In the residential case, the system's design allows owners to better cope with peak energy rates, occurring typically during the times from 5pm to 8pm. Due to the ice thermal storage, PV energy collected during times of peak solar radiation can be stored through thermal storage "ice", and thus can be accessed during peak energy rate hours. In the commercial sector, the system can

easily be scaled up. The difference is that PV modules will run the conventional HVAC system fully during work hours, and the ice thermal storage will be charged overnight, when energy rates are inexpensive. In both the residential and commercial cases, when the ice thermal storage is fully charged and there is no demand for cooling during daylight hours, excess PV power can be put back into the grid and sold to the energy provider.

Energy providers can also benefit from this system. The system was designed to use minimal grid energy during hours of peak energy demand, thus the peak power curve for power plants can be smoothed. Peak power generators are inefficient and not as cost-effective as base load systems. Creating a smooth, consistent energy profile enables power plants to become more efficient at providing energy. Thus by decreasing the need for peak power generators to be turned on, power plants can increase both their efficiencies and profit margins.

1:2 OBJECTIVES

Construction on the prototype HACS system started in 2011 as shown in Figure 1.1, at the Arizona State University Tempe campus, and was completed in early 2012. Prior to my involvement, Jonathan Sherbeck and Nate Sanford assembled the major parts for the prototype system during the summer of 2011. Taking Nate's place in the fall of 2011, I

assisted Jonathan in completing assembly of the system and installing the data acquisition instrumentation.

An economic model was constructed by Sadiq Jubran, which demonstrated the system's electrical and economic benefits in specific situations [5]. In order to show that this hybrid air conditioning system is not just a theoretical solution, a full prototype needed to be built. After completion of the construction of the prototype system, the main objectives of this project were outlined and are listed in table 1.1.

Table 1.1 Objectives

Install data collection devices on the system
Design of experiments
Error analysis
Coefficient of performance analysis
Thermodynamic modeling
System optimization

Numerous data acquisition devices needed to be installed in order to perform a proper analysis. Temperature, mass-flow, pressure and electrical measurements devices were installed. Design of experiments is a major subject for understanding how the data can best be collected from the system. Test scenarios were outlined and organized to make each test run provide the most valuable data. An error analysis on the instrumentation was required in order to make sure the data collected

were valid. From the experiments and data collected described below, a hypothetical analysis of the system's coefficient of performance (COP), cooling loads, and electrical power consumptions was performed. From further data collection, a full-study thermodynamic model could be constructed along with system optimization. Lastly, it is important to note that even though the system could not be subjected to rigorous testing, the hypothetical experimental analysis and outlined calculations nonetheless provide a model of how to compare such prototype systems to conventional HVAC units.

1:3 DESCRIPTION

The prototype hybrid air conditioning system (HACS), as shown in Figures 1.2-1.3, is a photovoltaic (PV) powered heating, ventilation and air conditioning HVAC unit combined with glycol thermal storage (ice).

Figure1.2 Top left: HACS prototype. Top right: Solar modules. Bottom left: Thermal storage. Bottom right: DC compressor and condenser

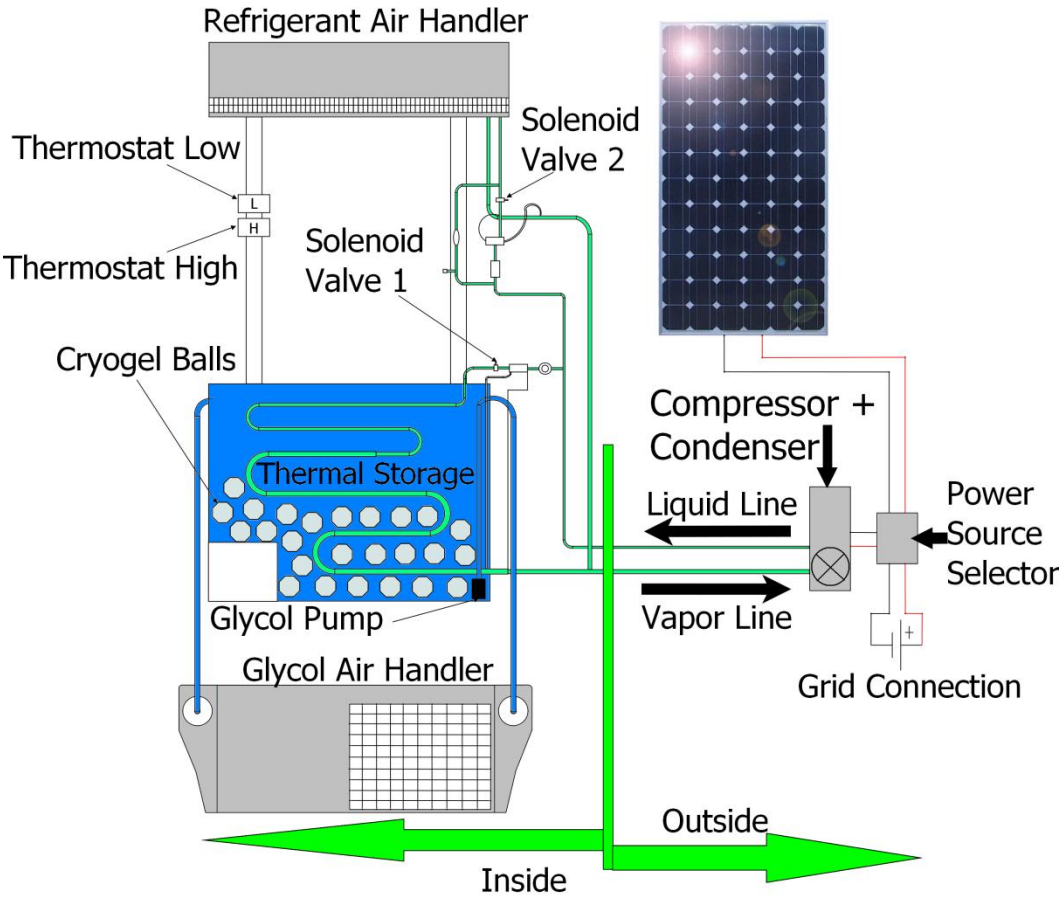

Figure 1.3 Prototype schematic

The prototype system consists of PV modules, a DC compressor, glycol thermal storage (0.284m^3 (75-gal) freezer filled with Cryogel balls, $9*10^{-4}m^3$ or 1 quart oil containers, $3.54*10^{-4}m^3$ or 12oz water bottles, immersed in 0.15m^3 of 40-gal of a weak glycol solution), two air handlers (a conventional 1 ton HVAC air handler and a glycol air handler) and a power selector box [1]. The glycol air handler was a custom design of combining a truck evaporator inserted into a custom hand-made air handler that allows for the air to pass three times over the evaporative coils upon exiting the air handler. The built system combines PV modules, paired with a direct current "DC" compressor cycling refrigerant (R134a)

through to separate evaporators. It is important to note that the use of a DC compressor allows for minimal energy loss from the energy harnessed from the PV modules. The two refrigerant loops connected to the compressor are as follows: the first loop is cycled through the conventional HVAC unit, and the second loop is cycled through the ice thermal storage, "the freezer." The flow of R134a is controlled by two separate solenoid valves, one valve at the inlet to the ice thermal storage, and the second one at the inlet to the conventional HVAC unit. The valve at the inlet to the thermal storage is programmed to be normally open while the second valve at the conventional HVAC air handler inlet is programmed to be normally closed. The solenoid valve states are controlled by two thermostats: one high-temperature thermostat and one low-temperature thermostat. The low-temperature thermostat controls the conventional HVAC side while the high-temperature thermostat controls the glycol thermal storage. When the room temperature is not within the programmed range of the low-temperature thermostat, the conventional HVAC loop is activated (solenoid valve 1 closes and solenoid valve 2 opens) and refrigerant is cycled through the conventional HVAC air handler. When the desired room temperature has been achieved, the solenoid valves return to their normal states, and refrigerant is cycled through the evaporator storing excess PV power within the freezer. During the peak energy rate hours (12-8pm), the PV modules run the entire

system until there is insufficient solar radiation. When there is not enough solar radiation to power the system, the DC compressor, and conventional HVAC unit are shut down. The high-temperature thermostat then controls the glycol air handler, cycling the glycol through the glycol air handler which in turn provides cooling power during the peak rate hours. The only systems that require electrical power during the peak rate hours are the glycol air handler and the glycol pump. The glycol air handler requires 200 W and the glycol pump requires 35W for a total of only 235W. In a final scenario, when temperature demands provide too great a load for one of the two air handlers, the HVAC air handler loop can be run with the glycol thermal storage air handler discharging the thermal storage at the same time, increasing the overall cooling power of the system.

As stated earlier, power is supplied either from the grid or PV modules. A power selector box was constructed as a device that differentiates which power source runs the HACS. Jonathan Sherbeck created an electrical box that is based on his own "two-diode theory." The two-diode theory consists of a simple setup of two diodes, one connected to the grid power, the other to the PV modules. The diodes differentiate between which power source runs the HACS. Thus, whichever power source is supplying the higher voltage runs the system. The inside of the box is shown in Figure 1.4, along with the full electrical diagram of the prototype system in Figure 1.5.

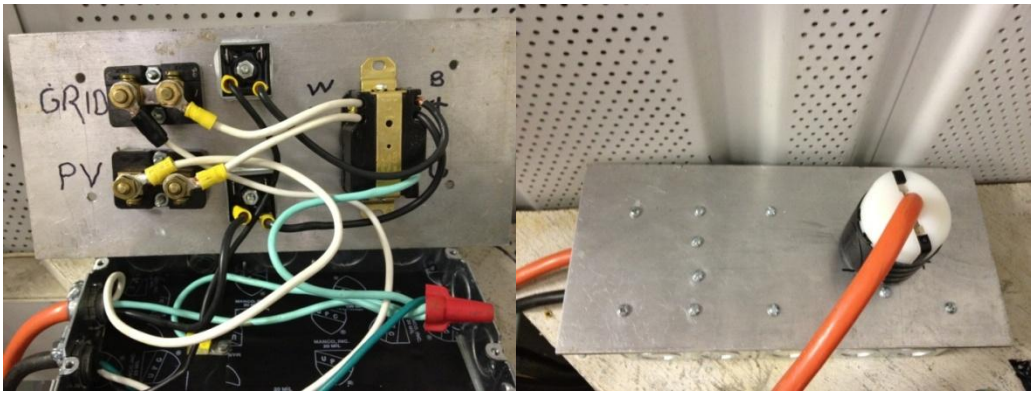

Figure 1.4 Power selector box, Left: Inside of box showing two diode theory, Right: Outside of the box

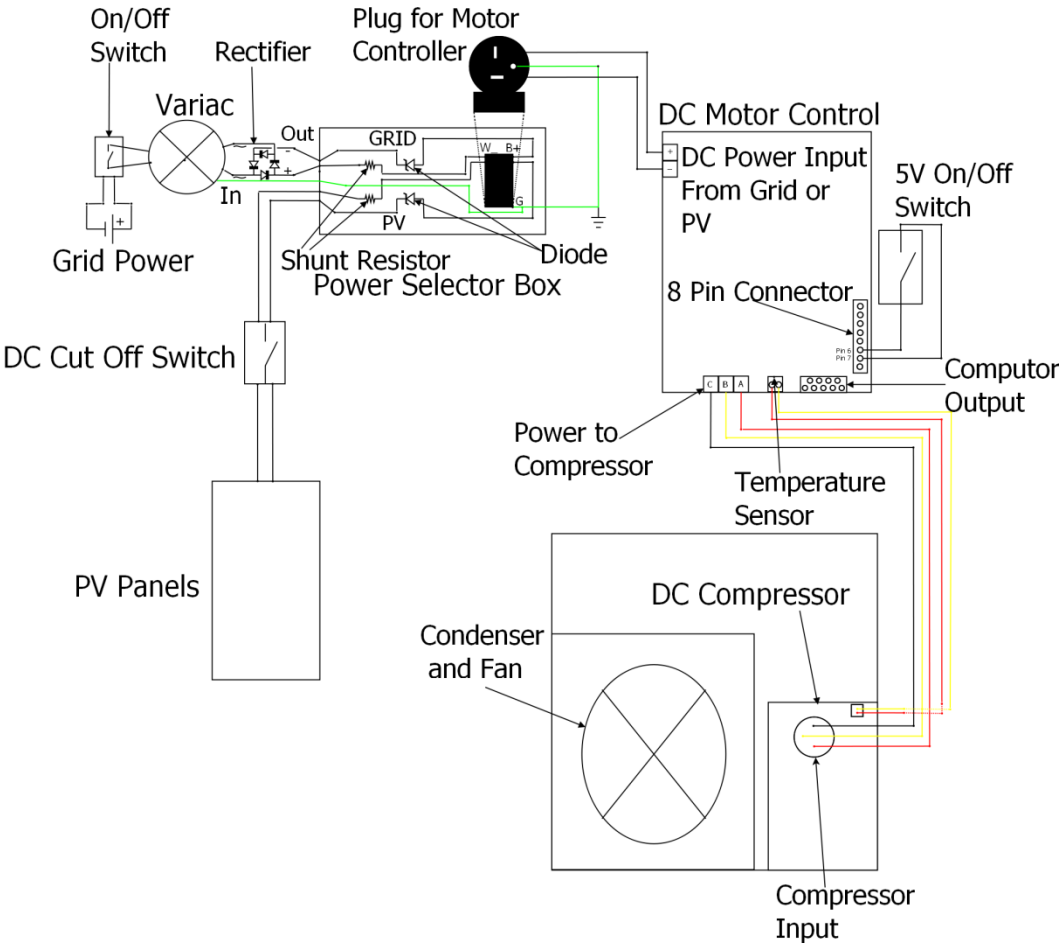

Figure 1.5 Electrical diagram of the HACS

The electrical diagram shown in Figure 1.5 illustrates that the grid power is first sent through a variac set at a specified voltage (120V). The alternating current (AC) is then sent through a rectifier and converted to DC. Then the power is directed into the power selector box. As shown in Figure 1.4, the grid power travels through its specified Zener diode, then to the plug that connects the power box to the DC motor controller.

On the PV side, the PV modules power is fed through a DC cut-off switch, which is then connected to the power selector box. Within the box the PV power is fed through its specified Zener diode and then to the plug outgoing to the DC motor controller. Note that the two shunt resistors within the box which take current measurements on the system have a claimed accuracy of ±0.25%.

Due to the PV modules supplying DC current to a DC compressor, power losses through an inverter do not occur. The only electrical power losses seen within the HACS system are when the grid AC power goes through the rectifier and is converted to DC, and that due to resistive power losses throughout the system. This system was designed to be highly energy efficient.

Chapter 2: BACKGROUND

2:1 VAPOR-COMPRESSION REFRIGERATION CYCLE

The proposed system includes a conventional air conditioning unit. This unit is operated using either the grid or the solar PV power, concurrently cycling refrigerant to cool either the indoor space or the thermal storage. As outlined earlier, the flow of the refrigerant is determined by the thermostat controls, and is based on the specific room temperature conditions.

This air conditioner uses a vapor-compression cycle to cool the space that is acting as the cold sink. In this case, the cold sink is the space that requires cooling and provides a cooling load to the air conditioner. It is necessary that it be colder than a separate space, the hot sink, for the vapor compression cycle to cool it. In this case, the hot sink is the outdoor, ambient air temperature.

The air conditioner works as a cycle, circulating a working fluid through its components in order to absorb and release heat as desired. This system is using R134a as the working fluid since that is the appropriate refrigerant to use for the compressor that was selected. The compressor uses DC power so that it can accept energy directly from the PV modules.

For this system, the compressor is located outdoors in the hot sink along with a condenser. The R134a is circulated through the compressor

and is compressed to a superheated vapor. The refrigerant is then condensed using a fan that blows ambient air across coils filled with the flowing refrigerant. This allows the refrigerant to release energy to the hot sink, the ambient air.

The refrigerant flows to an expansion valve inside the enclosed space which requires cooling, inside the building in this case. The temperature of the refrigerant drops as it goes through the expansion valve. The cooled refrigerant then flows through an evaporator, which consists of thin coil piping and is placed within the cold sink. This allows the refrigerant to absorb energy from the cold sink, which leaves the surrounding space colder. For air conditioning purposes, an air handler is used. The air handler blows air across the coils of the evaporator, dispersing the chilled air around the enclosed space and providing a continual supply of room-temperature air to be cooled by the evaporator. The evaporated vapor is cycled back outdoors to the compressor to release the stored heat from the enclosed space to the hot sink and continue the process [6]. Figures 2.1-2.2 portray the described vapor compression cycle.

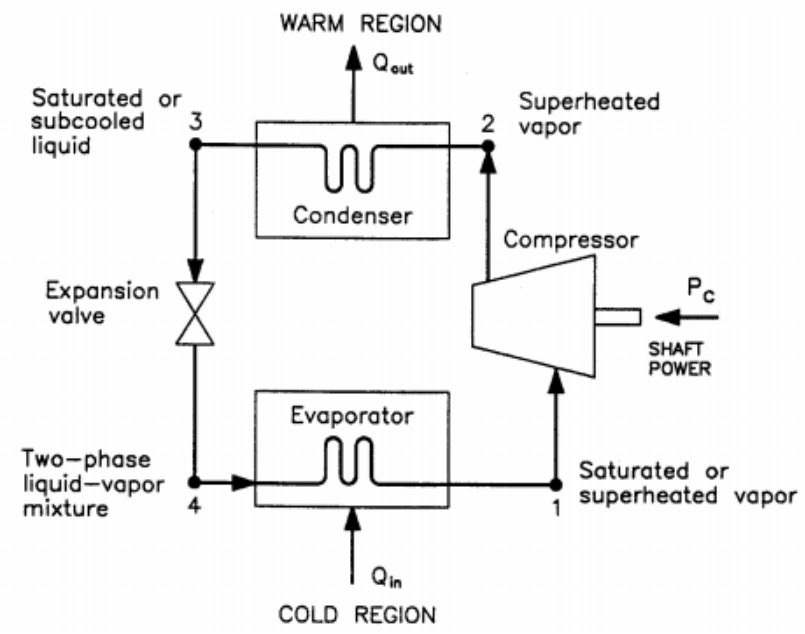

Figure 2.1 A vapor – compression refrigeration system [2]

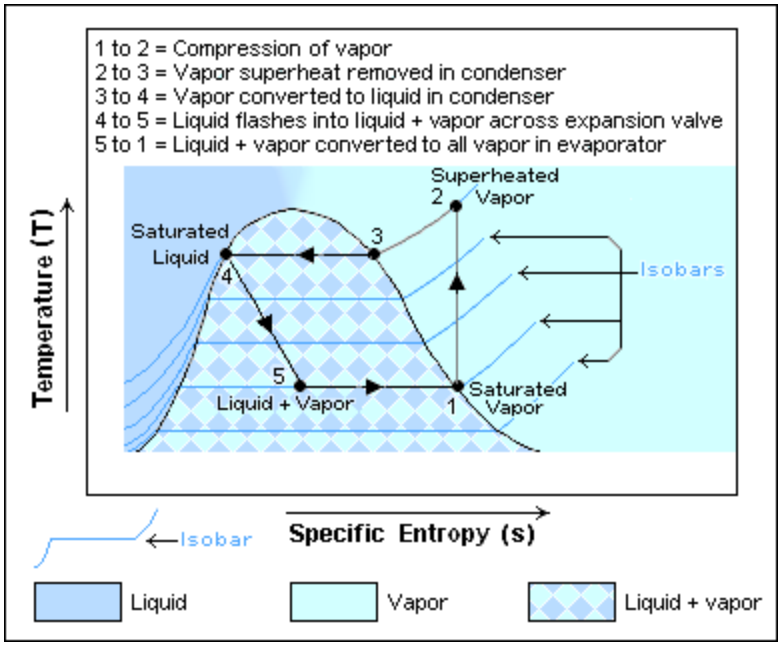

Figure 2.2 Vapor compression cycle, temperature vs. entropy diagram [7]

The described vapor compression cycles gives a good explanation for conventional HVAC systems. On the other hand, the HACS contains two evaporators and thus has two separate vapor compression cycles. Figure 2.3 displays the vapor compression cycle for the HACS.

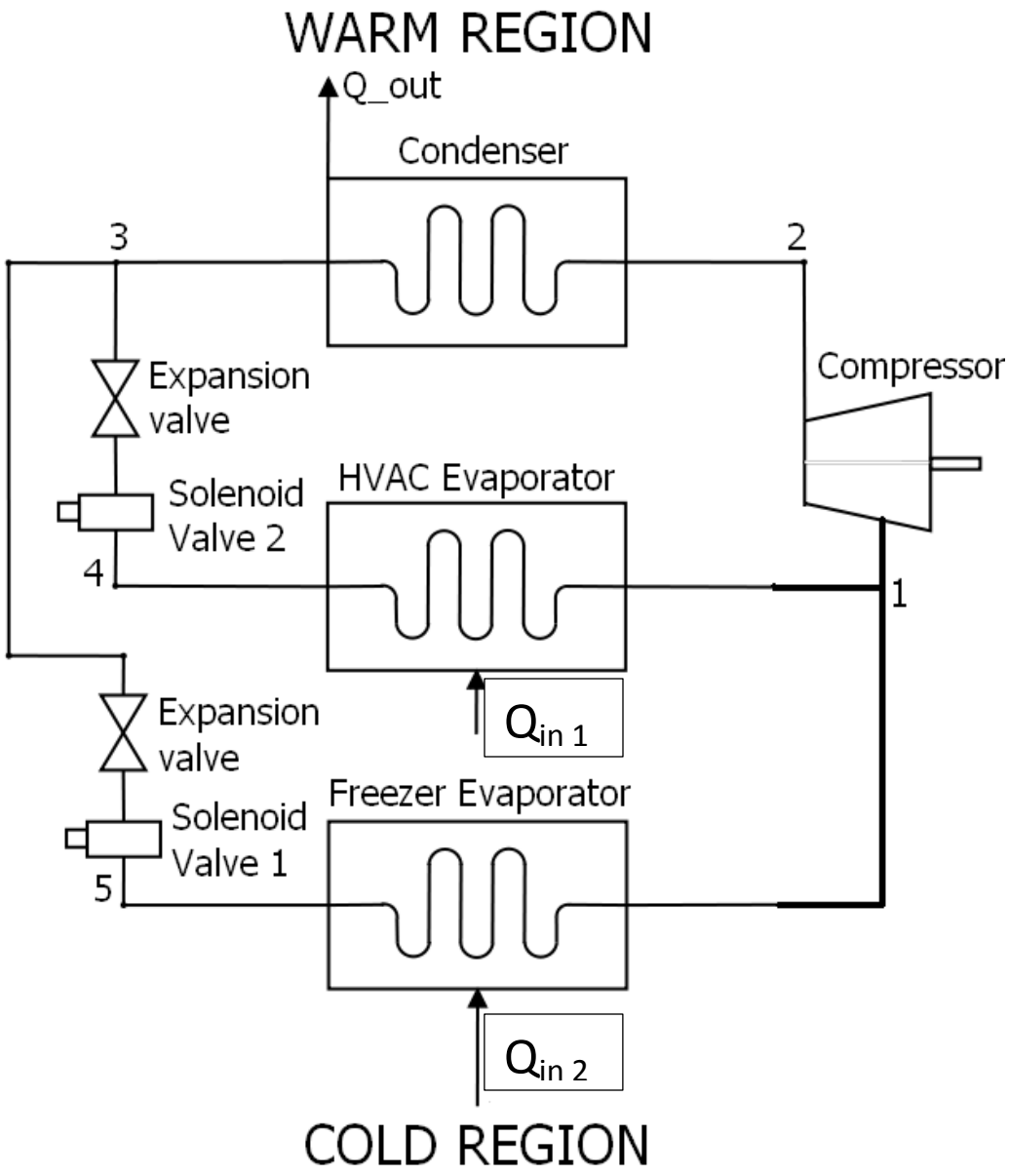

Figure 2.3 HACS vapor compression cycle

As seen in Figure 2.3, there are two vapor compression loops within the system. The first loop cycles through the conventional HVAC evaporator and consists of going from point 1→2→3→4 and back to 1. The second loop circulates the refrigerant through the evaporator within the freezer and consists of 1→2→3→5 and back to point 1.

Solar cooling can use two different methods. One method, a thermal-driven system, uses the heat provided by the sun to drive an absorption refrigeration cycle. Another method, used by our system, requires electrical or mechanical work input [8]. Our system, rather than using the thermal energy of the sun directly, uses the photovoltaic modules to convert sunlight to electricity, which is then used to power a refrigeration cycle, such as the vapor-compression cycle contained within the HACS [9].

While solar cooling can be provided without any storage capacity, our design is intended to make use of the high levels of sunlight during the peak irradiation time during the day in order to provide cooling during the subsequent period of peak cooling demand. Therefore, our design utilizes a method for storing energy for cooling as needed.

The conventional vapor-compression cycle is used to run R134a through a parallel section of the system into a separate expansion valve and evaporator. This evaporator is located in a thermal storage tank. A 0.284 m^3 (75 gallon) freezer chest functions as the thermal storage tank in our prototype. The refrigerant is run through four sets of identical expanding copper coils throughout the freezer, as shown in Figure 1.3. The start diameter of the coils is 0.0127m, and the ending diameter is 0.01905m. Each set of copper coils has an approximate surface area of 0.2662 m^2. The sum of the four copper coils is 1.066 $m^{2,}$ the total surface

area onto which energy transfer can occur from the refrigerant to the glycol solution.

In order to store the energy of the refrigerant, the evaporator is used to absorb heat from the contents of the thermal storage tank. A phase change in a substance is ideal for storing thermal energy, so water has been chosen due to its ready availability and lack of health hazards.

However, to utilize the thermal energy, some of the chilled contents of the tank must be extracted and used to absorb heat from the space that requires conditioning. As a result, containers of water are placed in the tank surrounding the evaporator coils. These containers are known as Cryogel Ice Balls, which are designed specifically for such applications [1]. They are sealed plastic balls containing water, and have dimples to allow them to easily expand when the water freezes. The Cryogel balls remain in the freezer, while a surrounding liquid absorbs the stored thermal energy from the balls as it passes over them, using the energy to cool the conditioned space by running through an air handler. Since it must remain in liquid phase at the freezing point of water, a weak propylene glycol-water solution has been chosen as a surrounding liquid; in addition to having a lower freezing point than water, it is less toxic than alternative substances. The solution within the freezer is a 5% glycol solution, which lowers the freezing point to approximately -1^{o}C or 30^{o}F and raises the boiling point to 101^{o}C or 214^{o}F.

The thermal storage tank is considered fully charged when the Cryogel balls are all completely frozen and the glycol solution is at its freezing point, frozen near the evaporator, but still in liquid state so that it can flow between the inlet and outlet of the thermal storage tank, cycling through the glycol air handler.

Alternate containers for holding water in the thermal storage tank were also explored. Recycled water bottles or $9.4*10^{4}$ m^{3} (1 qt) oil containers also effectively isolate water from the surrounding glycol solution while allowing a sufficient heat transfer. Water bottles, although much more cost effective and more readily available, are less durable and tend to leak. The used oil containers need to be thoroughly washed in order to remove any oil residue that could contaminate the thermal storage solution. Cryogel balls were specifically designed to operate under the temperatures and pressures of the storage tank, and were specially made to allow for expansion when liquid water turns to ice. Depending on the dimensions of the thermal storage container and the evaporator coils, either the Cryogel balls or the water bottles may be preferable for optimum packing, due to their different geometries.

2.2 OPERATIONAL MODES

Programmable thermostats control the states of the solenoid valves, which in turn control the path of the refrigerant through the two refrigerant loops as shown in Figure 1.3. When the temperature of the conditioned space is higher than the programmed set point, solenoid valve 2 (normally closed) opens and solenoid valve 1 (normally open) closes, directing the refrigerant into the conventional air handler to cool the room. The two main operational settings of the HACS are as follows: off-peak energy rate hours and on-peak energy rate hours. Between these two settings there are three subdivision modes, equaling a total of six separate modes. These modes of operation can be viewed in table 2.1. and Figure 2.4, which display the feedback loops for the 6 different operational modes that the HACS offers.

Table 2.1 Operational modes

Modes	Powered Equipment	On-Peak Energy Hours	Off-Peak Energy Hours
Cooling modes			
1	Compressor cycling refrigerant to HVAC air handler	N/A	Available
2	Compressor cycling refrigerant to HVAC air hander, thermal storage discharging through its respective air handler	N/A	Available
3	Thermal storage discharging through its respective air handler	Available	Available
charging modes			
1	Compressor cycling refrigerant to the thermal storage evaporator	N/A	Available

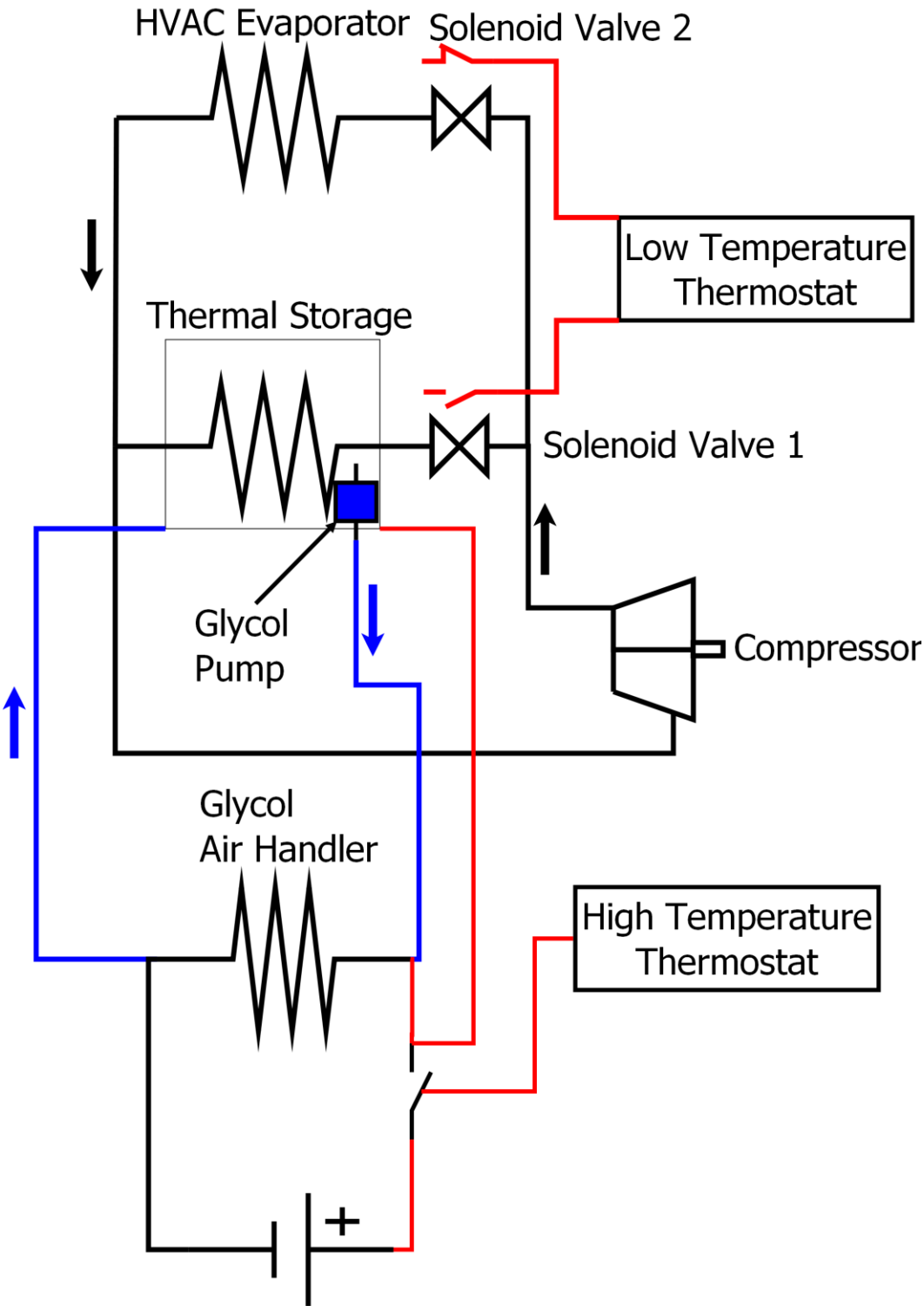

Figure 2.4 HACS control diagram

The two thermostats in Figure 2.4 control the operation of the HACS. Figure 2.4 illustrates how the low-temperature thermostat controls the refrigerant flow to either the thermal storage or the conventional HVAC air handler. Solenoid valve 1 is normally open and solenoid valve 2 is normally closed; thus the normal refrigerant loop cycles through the thermals storage. When the room temperature is above the input setting of the low-temperature thermostat, the two solenoid valve states are switched, diverting refrigerant flow to the HVAC air handler, providing cooling. The high-temperature thermostat controls the power to the glycol pump and air handler. The normal state of the switch is open, thus the pump and air handler are off. When the high-temperature thermostat reads a higher temperature than what the user has selected, the switch closes and the glycol pump and air handler are powered on. It is important to note that using thermal storage allows the size of the conventional air conditioning unit to be smaller, because the glycol air handler can be turned on and run using the stored cooling if the conventional air handler does not cool the room to the programmed temperature. Thus, the second air handler can supplement the cooling power of the first.

Other technologies are sometimes utilized to store or use energy during low-cost off-peak times. Batteries can be charged during this period, or other technologies can be used for storing thermal energy. For

example, water heaters and chillers are sometimes run during the night to store the heated or chilled water until it is needed during the day, rather than using the electricity needed during the day at higher costs [10]. A good example of this type of system is the Ice Bear by Ice Energy. This system uses off-peak low-cost nighttime grid energy to freeze ice around refrigerant condensing coils. During daytime hours, the refrigerant can be cooled within the coils contained in the ice and run back through an evaporator to provide cooling [11].

Energy generated through photovoltaic power is commonly used directly, without being stored. Our system uses the photovoltaic power directly, with as few losses as possible, by converting it directly to its end state of thermal energy without doing conversions in between, and storing it when it does not need to be used immediately as well as storing off-peak grid power. This avoids using on-peak grid power, and problems associated with storing power in a battery in the form of electricity. It also avoids the problem that sunlight is not consistent and not always available during on-peak times and periods of high cooling demand, such as during early evening.

The Ice Bear is a somewhat comparable technology currently on the market; it is designed for freezing water during off-peak times. The Ice Bear uses a conventional air conditioner as necessary, except during on-peak times, when it circulates refrigerant through the ice and into an

air handler to cool the conditioned space. This competing system is described in the next sub-section.

2:3 ICE BEAR

Ice Energy, a Colorado-based company developed another thermal storage system known as the "Ice Bear." The company describes the Ice Bear system as,

> "An intelligent distributed energy storage solution that works in conjunction with commercial direct-expansion (DX) air-conditioning systems, specifically the refrigerant-based, 4-20-ton packaged rooftop systems common to most small to mid-sized commercial buildings [11]."

The Ice Bear system, as shown in Figures 2.5 and 2.6, consists of a 450-gallon container filled with water and copper piping, with an external compressor, condensing unit, and air handler [11],[12]. The system is designed to use low-cost nighttime (6pm-6am) grid power to charge the ice thermal storage. During morning hours (6am-12pm) the conventional air conditioning unit is driven. Through peak energy rate hours (12pm-6pm) the compressor and condensing unit are turned off and the refrigerant is cooled by being pumped through the ice storage and circulated back to the air handler to provide cooling until the ice has

melted. The cycle repeats itself every day. Ice Energy claims that the system can "deliver an average reduction of 7.2kW of source equivalent peak demand for a minimum of 6 hours daily, shifting 32 kW_{th}-hours of on-peak energy to off-peak hours." [11]

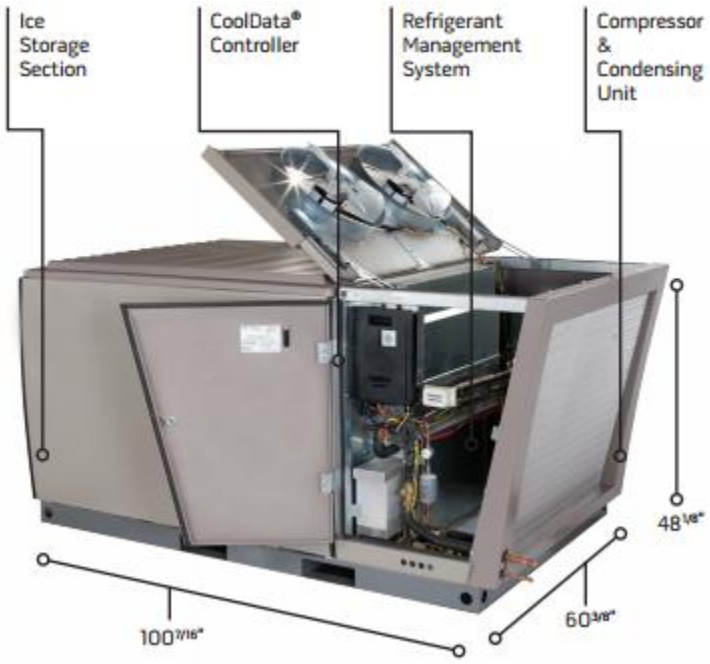

Figure 2.5 Ice Bear [11]

Figure 2.6 Ice Bear thermal storage [13]

2:4 COMPARISON BETWEEN THE HACS AND THE ICE BEAR

The prototype hybrid air conditioning system (HACS) and the Ice Bear have both been constructed with the intent of reducing net energy consumption. Similarly, both systems at full scale deployment also possess the ability to improve electric system load factors, thus reducing electric system costs and increasing global efficiency. While both systems are built to combat similar complications, each system goes about this in a unique manner. The Ice Bear system helps reduce peak energy demand through taking advantage of low-cost nighttime energy to charge the ice storage for daytime use. Similarly, the HACS takes advantage of off-peak energy to power the system, but it does this during the day as well as at night, and has the ability to be completely driven off of PV modules, with excess PV power being stored in the form of ice energy.

Comparing the similarities and differences between the HACS and Ice Bear system illustrates the advantages of the HACS prototype. Table 2.2 is a cost comparison of the major mechanical parts for both the HACS and Ice Bear.

Table 2.2 HACS vs. Ice Bear cost analysis. *Individual part costs were unattainable due to system being sold as a complete package [12]

HACS	Price	Ice Bear 5 ton unit	Price
1 ton DC Compressor and Condensing Unit	$ 675.00	4.3 ton Copland Scroll Compressor	$ -
Motor Controller	$ 819.00	CoolData® SmartGrid Controller	$ -
Thermal Storage Temperature Controller	$ 200.00	Refrigerant Management System	$ -
2 Solenoid Valves	$ 250.00	420 gal ice storage	$ -
HVAC air handler	$ 440.00	HVAC air handler	$ -
Glycol Air handler	$ 440.00	Thermostat	$ -
Variac	$ 222.00		$ -
2 Thermostats	$ 100.00		$ -
75 gallon freezer	$ -		$ -
PV modules	$2,930.00		$ -
Total Unit Price	$6,076.00	Total Unit Price*	$12,000.00

As shown in Table 2.2, the prices of the Ice Bea can be hard to compare to the HACS cost. The smallest system of Ice Bear available is a 5-ton unit. With extrapolation, the 5-ton unit comes out to cost approximately $2,400/ton; a 2-ton unit would cost approximately $4,800. The HACS is a 1-ton unit that has a 2-ton cooling capability when both air handlers are running. The HACS system costs a total of $6,076.00, which is $1,276.00 more than the equivalently-rated Ice Bear system. It is important to note that even though the initial price of the HACS may be higher, the energy the system saves will likely have greater value in the long term. Additionally, in order to get a true understanding of the cost comparison, it is important to compare the retail price of the two systems. With an estimated retail markup of 50%, table 2.3 shows the new cost comparisons.

Table 2.3 Markup costs

	HACS	Ice Bear
System Size	1-2 ton	5 ton
Cost prior to markup	$6,076.00	$ 8,000.00
Markup cost	$9,114.00	$12,000.00

Looking at table 2.3, one could recalculate the cost per ton of the HACS system to obtain $4,557 per ton. At the present time, it is clear that the HACS system is more expensive per ton than the Ice Bear. However, it is important to consider the fact that the Ice Bear system has already undergone thorough prototyping and analysis. The system is sold as a complete package; discounts on parts may be offered. After going through its own rigorous packaging analysis and subsequent high volume production scale, the price of the HACS system would presumably decrease to a comparable level.

When considering the overall size of the two systems, the HACS system can be smaller due to its ability to use the thermal storage along with the conventional HVAC air handler at the same time. The Ice Bear, which only consists of refrigerant lines, has to be larger because it can only use one source of cooling at a time, i.e., the conventional HVAC side or the ice storage. It is important to note that there would be a slight increase in price if the HACS system were scaled up by increasing the compressor capacity and ice thermal storage size to match the 4 ton capacity of the Ice Bear. The price increase, however, would only be on

the order of approximately $200. Thus, it is important to realize that since the HACS system can achieve the same cooling power as the Ice Bear while running a smaller compressor, it can run at a higher efficiency and consume even less electricity. Table 2.2 compares the characteristics of the HACS vs. the Ice Bear.

Table 2.4 HACS vs. Ice Bear capacities [11]

	HACS	Ice Bear
Cooling load (tons)	1 to 2	5
Unit Price ($)	$ 6,076.00	$ 12,000.00
Price / ton ($)	$ 3,038.00	$ 2,400.00
Predicted thermal storage ability (ton-hours)	1 ton for 12 hours	5 ton for 6 hours
Ability to provide heat	Yes	No
Ability to run off PV power	Yes	No
Ability to feed power back to grid	Yes	No
Ready for off grid use	Yes	No

Chapter 3: EXPERIMENTAL METHODOLOGY

3:1 DESIGN OF EXPERIMENTS

In order to study the efficiency of the HACS prototype, a complete design of experiments (DOE) had to be performed. The HACS was designed in order to decrease the energy consumption and increase the operating efficiency of cooling units in forward operating bases and commercial and residential buildings. An experiment designed to show the operating efficiencies and benefits of the HACS was constructed.

Following the basic procedural steps of DOE, independent, dependent, and constant variables were assigned [14]. Table 3.1 displays the list of variables that were derived.

Table 3.1 List of Variables *Constant variables are dependent on which independent variables are held constant for a specific experiment

Independent Variables	Dependent Variables	Non-Manipulated Variables	Calculations
Compressor RPM	Energy used to charge the thermal storage	Outside temperature	Cooling power of HVAC air handler
Glycol Flow Rate	Energy required to run the system	Solar radiation	Cooling power of glycol air handler
Room temperature / Load	How long TS lasts before complete discharge		Cost of grid power / Energy savings
Glycol air handler fan speed	Max cooling power		COP of system
Time of day	Room temp over time		Load on HACS vs. Room temperature
			PV power consumed vs. supplied

The list of variables in Table 3.1 is the basis upon which the experimental procedure was constructed. It is important to note that the constant variables will change from experiment to experiment as different independent variables are held constant. The four independent variables, compressor RPM, glycol flow rate, room temperature/load, and the glycol air handler speed allow for four general test procedures to be assembled. The four test tables, along with test 1 procedure are provided in appendix A. By changing the four independent variables described above, a clear and concise understanding of how the HACS system operates may be gained.

3:2 TESTING

As discussed previously and in better detail in appendix A, test 1 was to be performed on the hybrid air conditioning system first until the compressor failure. The independent variable selected was room temperature/load. This test allowed for the greatest and most general observations to be made with clear precision and accuracy. Test 1, as described in appendix A, consists of running a four-day test cycle with the high and low thermostats set to specific temperatures (the high temperature thermostat set to 296K or 73^{o}F and the low temperature thermostat set to 295K or 72^{o}F). The first run of the test was performed with the thermostats set at common household temperatures for summertime [15], [16]. The test was then planned to be repeated until a

range of 66-80^{o}F had been covered. Through running this first test procedure, calculations and observations could be performed on the following: coefficient of performance (COP) of the HACS, cooling power of both the glycol and conventional AC air handler, load on the HACS vs. temperature, PV power consumed vs. supplied from the grid and the cost of grid power and or energy savings for the HACS. Other observations that could be made consisted of how long the glycol thermal storage took to become fully charged and discharged. The cooling power of the thermal storage could be observed over time, with day four of the test being specifically designed to show the glycol thermal storage's effectiveness. This last test, along with the other three tests, would allow a clear observation of how long the PV modules can run the HACS during daylight hours.

The second test set to be performed on the HACS system was to vary the glycol thermal storage flow rate through its air handler. Regulating the glycol flow rate is as simple as varying the diameter of the glycol inlet tube. The second test spans a two-day period. Day one is used to run the HACS system until the glycol thermal storage is fully charged. On day two, the glycol thermal storage is fully discharged. This test allows for observations to be made on how to optimize the discharge of the glycol thermal storage while maintaining an optimal cooling power across the glycol air handler.

Test 3 is designed to show the heat transfer properties of the overall HACS system, but most importantly within the glycol thermal storage. By varying the compressor revolutions per minute (RPM) rate, observations could be made on how quickly and efficiently the thermal storage could be charged. Another aspect to varying the compressor RPM, observations on power required to run the system versus compressor RPM could be made, allowing for further optimization of the HACS.

The final test consists of varying the fan speed of the glycol thermal storage air handler. Through varying the speed of the glycol air handler fan, the cooling power can be observed with respect to fan speed. Through running this test and observing the previous results from test 2, one could observe and calculate the most efficient way to discharge the thermal storage, while at the same time maintaining a level of cooling power that would meet the temperature needs of the operator. Through running tests 1-4, a clear understanding of the HACS prototype could be garnered, and system optimization could be completed. Ultimately, the HACS system could be re-built or manufactured and scaled to specific user requirements. Finally, it is important to note that these tests were designed specifically for the first HACS prototype (the DC powered system). Due to the event of the compressor failure, a new prototype system is under construction that will be an AC-powered system. Thus,

the tests outlined above provide a solid foundation for future testing of a second HACS prototype.

3:3 SYSTEM SETUP

To gain a complete understanding of our hybrid air conditioning system, and run the previously discussed test procedures, extensive test equipment had to be installed. Tables 3.2 through 3.5 list the equipment used in the construction of the prototype system, including the total installed instrumentation and what it was paired with for data collection.

Table 3.2 HACS parts and corresponding test equipment

Parts	Manufacturer / Part No.	Inserted Test Equipment
10 PV modules	Solar Cemiconductor Put Ltd	
DC cutoff switch	SQUARE D	
Variac	STACO Energy Producs	
Power selector box	Custom Built	2 voltage / 2 current sensors
High temp thermostat	LUX TX500E	1 thermocouple taped on
Low temp thermostat	LUX TX500E	
DC compressor	Masterflux SIERRA05-0982Y3	
Outdoor condenser	Masterflux	
DC motor controller	Masterflux 025F0062-01	
Refrigerant inlet line	OD = 1.3cm	Pressure transducer / Rotameter / Thermocouple
Refrigerant outlet line	OD = 1.9cm	Pressure transducer / Thermocouple
HVAC air handler	Air Con ACN1318HPCCOEV	
2 solenoid valves	Parker 6B05	
Freezer for thermal storage	Recycled	9 Dispersed thermocouples
Thermal Storage Evaporator	Custom Built 1.3cm ODouter to 1.9cm OD	
Cryogel balls	Cryogel	
12 Oz water bottles	Recycled	
1 quart oil containers	Recycled	
Weak glycol solution	Sierra Antifreeze	
Glycol pump	Via Aqua VA-306	
Glycol inlet line	1.9cm ID	Thermocouple
Glycol outlet line	2.5 cm ID	Rotameter / Thermocouple
Glycol air handler	Custom Built	

Table 3.3 10 Solar module part numbers

Solar Cemiconductor Put Ltd
S2-6M313909-0357747
S2-6M313909-0357743
S2-6M354109-0357732
S2-6M354109-0357741
S2-6M313909-0357748
S2-6M313909-0357745
S2-6M354109-0357734
S2-4M154109-0357726
S2-4M154109-0357719
S2-4M154109-0357718

Table 3.4 Sensor manufacturer information

Sensor	Manufacturer / Part No.
Glycol rotameter	King Instruments K72-7/1
Refrigerant rotameter	King Instruments 2-32-G-042
Thermocouples	OMEGA engineering K-type
Shunt resistors	MLA-15-50 0-15A
Pressure Transducers	Setra 209
Sensor data acquisition device	National Instruments SCB-100

Table 3.5 Total test equipment

Total Test Equipment	No. of Sensors
Rotameters	2
Thermocouples	14
Voltage	2
Current	2
Pressure Transducers	2

In order to be able to perform analysis on the cooling power, coefficient of performance, electrical power consumed, and load on our system, many measurement devices were considered. To execute these calculations, measurements of the refrigerant and glycol flow rate, pressures within the refrigerant lines and many temperatures needed to be collected. Also current and voltage sensors needed to be placed on both the PV and grid side in order to observe the overall power distribution and consumption of our system. Figure 3.1 shows the locations within the HACS system in which testing equipment was installed.

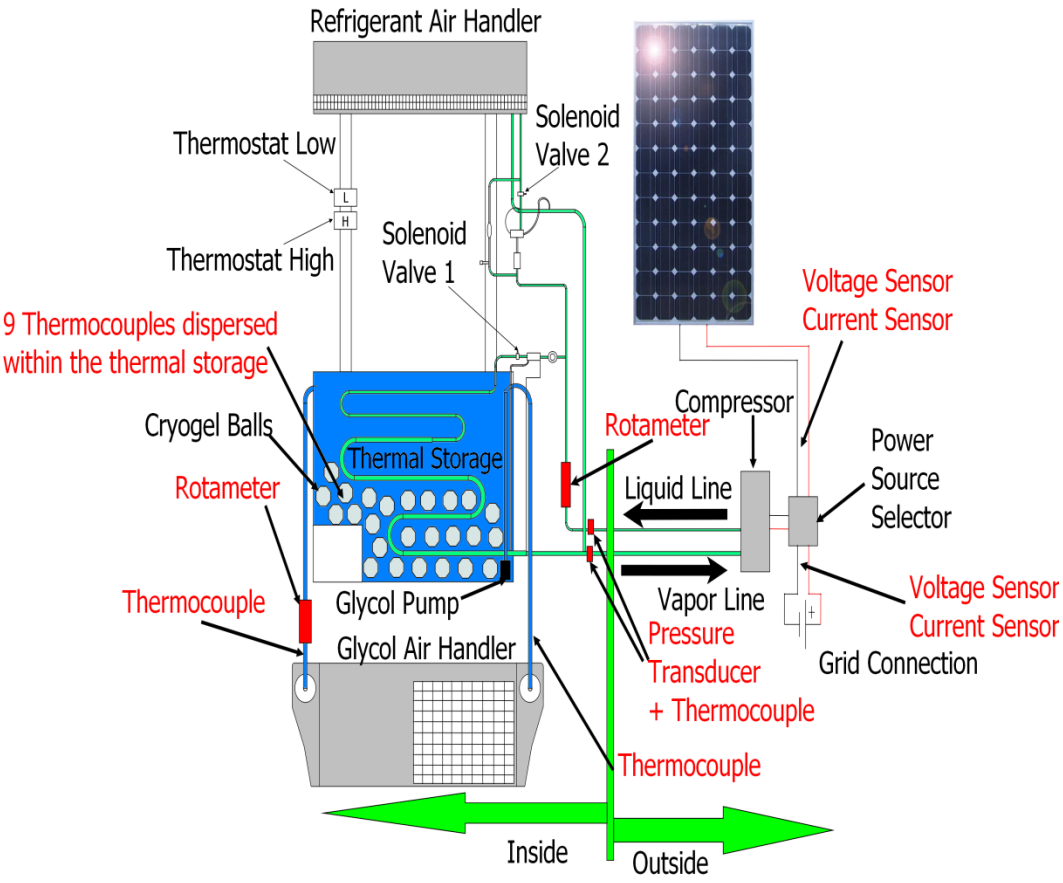

Figure 3.1 Test equipment

As shown in Figure 3.1, there are two rotameters, one to measure the refrigerant flow rate, and one for the glycol flow rate. Pressure transducers have been placed on the inlet and outlet refrigerant lines across the compressor. Thermocouples were placed at the inlet and outlet of both the AC and glycol air handler along with nine thermocouples within the glycol thermal storage. Also current and voltage probes were installed on the PV and grid side of the system.

All of the experimentation equipment except both rotameters output an analog signal that could be wired to a sensor data acquisition device. A LabVIEW program was written to compile all the data and compute some of the calculations. Figures 3.2 and 3.3 show the front panels of the LabVIEW program.

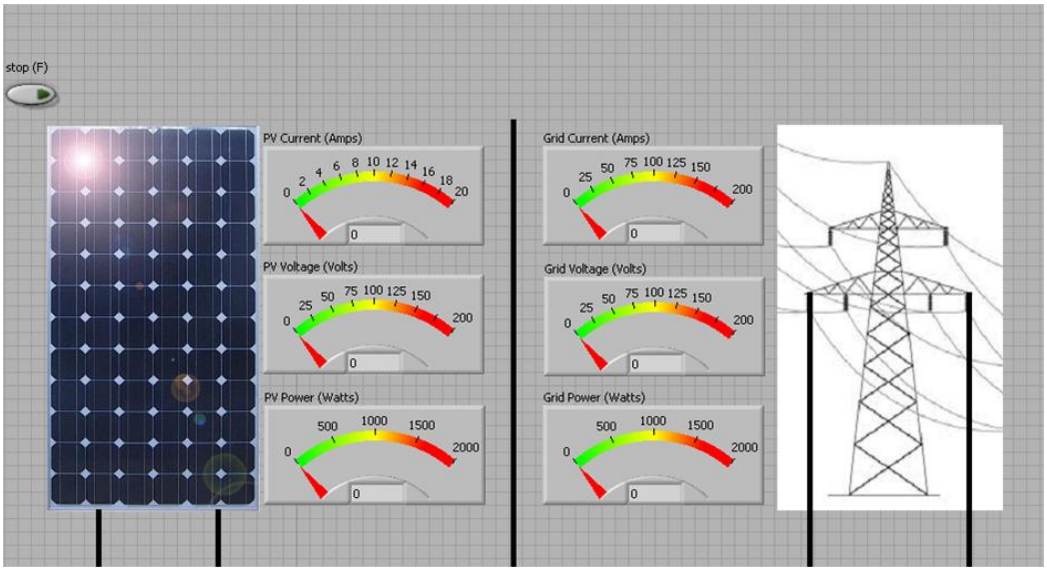

Figure 3.2 LabVIEW front panel 1

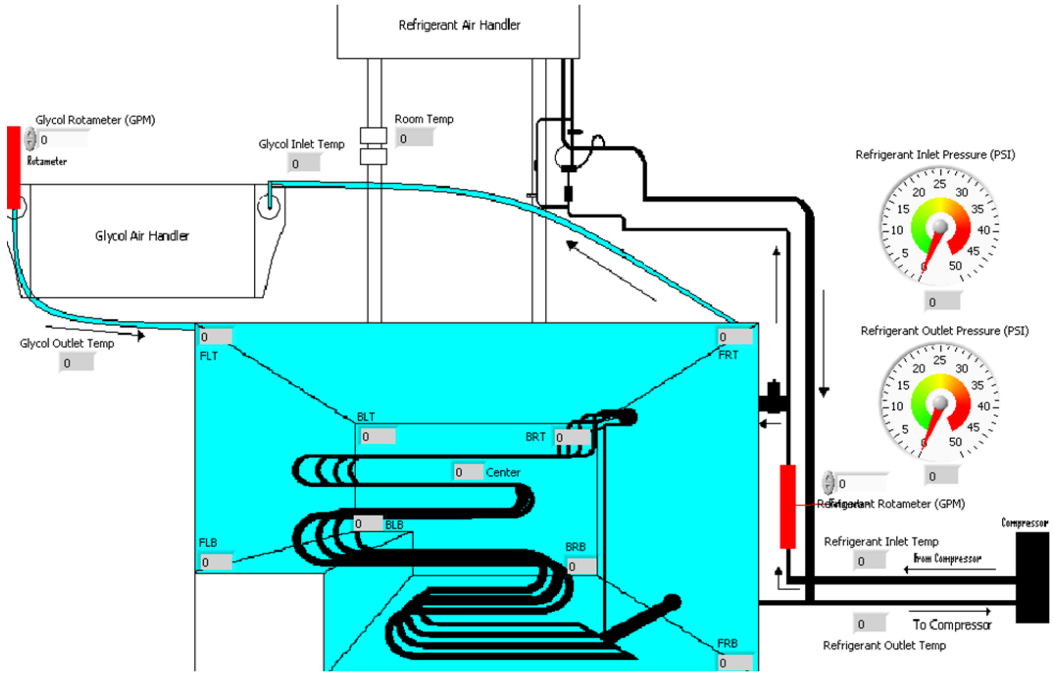

Figure 3.3 LabVIEW front panel 2

The LabVIEW front panels were designed to give a simple overview of how the hybrid air conditioning system presently functions. The program compiles the data with respect to time and saves it as an Excel file where further calculations could be completed.

As described earlier, the HACS prototype has four different modes of operation; 1) compressor running refrigerant to the AC air handler, 2) compressor running refrigerant to the glycol thermal storage, 3) glycol thermal storage cycling through the glycol air handler (compressor, and AC air handler are off), 4) compressor cycling refrigerant to the AC air handler, with the glycol thermal storage cycling through its respective air handler. It is clear to see that the HACS has many modes of operation and can constantly change which mode it is running in.

The ability of the HACS to constantly change state made it important to collect data continuously with respect to time. The LabVIEW program was created to sample data at a rate of once per 10 seconds. This 10 second interval was specifically selected because it allows observation of constant changes in system function, while avoiding collection of redundant data.

3:4 SOUGHT OBSERVATIONS AND CALCULATIONS

As described earlier, if the four outlined tests were carried out, they should provide data that can be used to calculate the following: energy used to charge the thermal storage, energy required to run the system, how long the PV modules can run the system daily, how long the thermal storage effectively lasts, performance of system with different room temperature loads, cooling power of both air handlers and the max cooling power of the system. From the data collected, each discussed observation and calculation could be performed.

3:5 EXPLANATIONS OF CALCULATIONS

In order to calculate the energy used to charge the thermal storage timed data on the average temperature throughout the thermal storage, inlet and outlet temperature of the refrigerant lines, mass flow rate of the refrigerant, and electrical power consumed by the HACS system need to be collected. The collected data can be inserted into equation 1 to calculate the total heat removed by the evaporator within the

conventional HVAC air handler and the glycol thermal storage evaporator [17]:

$$Q = m(\Delta h_{ref}) \qquad (1)$$

where Q is the total heat load (kW_{th}), m is the mass flow rate of the refrigerant ($kg\ s^{-1}$), and Δh_{ref} is the enthalpy change of the refrigerant (J). With the previous calculations, the power used to charge the thermal storage and efficiency of charging the thermal storage can be studied.

The energy required to run the system can be analyzed through collecting the current and voltage data supplied by the solar modules and grid over time. These data can be compared to the faceplate data on each electrical device within the HACS system, in order to compare the actual power requirements of the HACS versus the additive nameplate power requirements. With this comparison the overall electrical efficiency of the system may be calculated through dividing the measured power $W_{measured}$ over the theoretical nameplate power $W_{theoretical}$, where $W_{measured}$ is the supplied power from the solar modules and grid, and $W_{theoretical}$ is the summed faceplate power requirements of each electrical part of the HACS. The data collected on the total power supplied by the grid and PV modules (kWh) can be used to calculate the cost to run the HACS and the savings that it generates ($/kWh).

At the present time, the two-diode selector box as described in previous sections only allows our PV modules to run our system when

their output voltage is greater than the grid voltage. However, the DC compressor can run on a minimum voltage of 90V. Therefore, it is obvious that our PV modules may at times be supplying enough power to run the system, but may not be in use. By attaching an external load to the PV modules, the current and voltage can be measured during the times when the PV modules are not powering the HACS. Through collecting the power measurements of the PV modules over the course of time, it will become clear how many hours a day the PV modules can actually run our system during different times the year, along with how much power it can feed back into the grid.

Since the hybrid air conditioning system is basically a heat pump, the performance of the system can be directly calculated using an equation for coefficient of performance (COP). The COP of a conventional HVAC unit can be calculated using equation 2 [2]:

$$COP = \frac{\frac{Q_{in}}{m}}{\frac{P_c}{m}} = \frac{h_1 - h_4}{h_2 - h_1} = \frac{Q_c}{W} \quad (2)$$

where Q_{in} is the heat transfer rate or refrigeration capacity (W), Q_c is heat removed from the cold reservoir (J s^{-1}), P_c is the input power as mechanical power at the shaft of the compressor (W), m is the mass flow rate (kg/s), and $h_{1\text{-}4}$ is the specific enthalpy per unit mass (J/kg) at the specified point in Figure 2.1, and W is the work consumed by the heat pump (J). Because the HACS prototype contains two evaporators, the

conventional COP equation does not apply to the system. In order to calculate the COP of the HACS both evaporative loops need to be taken into account. The COP of the two separate evaporative loops can be explained by Equation 3:

$$COP_{conventional\ loop} = \frac{h_1 - h_4}{h_2 - h_1}, COP_{thermal\ storage} = \frac{h_1 - h_5}{h_2 - h_1} \quad (3)$$

In Equation 3, $h_{1\text{-}5}$ represents the specific enthalpy per unit mass (J/kg) at the specified points in Figure 2.3. Equation 3 is only useful for explaining the COP of the HACS when it is functioning in either of the two modes. In order to obtain a COP that represents the system as whole, it would be important to compute the two COP calculations in Equation 3 with respect to time (24 hr cycle). Using the last expression of Equation 2 and adding index notation to represent the different cycles of the HACS, the COP as a whole may be represented as Equation 4:

$$COP_{HACS} = \frac{\int_0^{time} \frac{Q_{i\ grid>0} + Q_{i\ PV>0}}{W_{grid+PV}}\, dt}{time} \quad (4)$$

where Q is the heat removed from the room (W), W_{grid} *and* W_{PV} is the power provided by the grid or PV modules (W), time is the hours of operation (h) and i represents the three modes of operation (1-3) defined as: 1) compressor running refrigerant to the HVAC air handler, 2) compressor charging the thermal storage, 3) thermal storage discharging. The sum of the three separate COP's calculated from the three modes of

operation is divided by the power input to the system. This whole term is then integrated with respect to time in order to get an average COP for the HACS. It is also important to note that the integral boundaries can be adjusted to fit different time periods such as months, days or even years.

The freezer that the glycol thermal storage is contained in is an excellent insulator, thus allowing for the thermal storage to stay at freezing temperatures for long periods of time. When the thermal storage is being used for cooling purposes, circulating the glycol solution through its perspective air handler, the cooling power can be calculated using Equation 5 [3]:

$$Q = V\rho c_p \Delta T \tag{5}$$

where Q is the total heat load (kW_{th}), V is the volumetric flow rate of the glycol ($m^3\ s^{-1}$), ρ is the density of the weak glycol solution (kg m^{-3}), c_p is the specific heat (J $kg^{-1}\ {}^oC^{-1}$), and ΔT is the temperature difference across the inlet and outlet refrigerant lines (^oC) [13].

In order to observe and calculate the effective period of time that the thermal storage lasts, it is important to observe the cooling power of the glycol air handler with respect to time. The glycol thermal storage will be deemed effective as long as the cooling power across the glycol air handler is ≥0.

Taking temperature measurements at the inlet and outlet refrigerant lines, the mass flow of the refrigerant with corresponding

R134a specific heat and density properties will be enough information to calculate the conventional HVAC air handler cooling power. To obtain the cooling power of the glycol air handler, temperature measurements across the air handler, the mass flow of the glycol through the air handler and the specific heat and density of our ice thermal storage solution will provide ample numerical data.

The maximum cooling power of the system is represented as the sum of the two air handlers' cooling power, as shown by Equation 6:

$$Q_{max} = Q_{conventional} + Q_{glycol} \quad (6)$$

Q_{max} is the additive cooling power (kW_{th}), $Q_{conventional}$ is the cooling power of the conventional HVAC air handler (kW_{th}), and Q_{glycol} is the cooling power of the glycol air handler (kW_{th}). Note that the maximum cooling power can be taken with respect to time as the glycol thermal storage is discharged.

With the collection of abundant measurements, the overall functionality, performance, and advantages of the HACS can be observed and calculated. The economic modeling performed by Sidiq Jubran can be compared and confirmed with the test data and calculations [5]. A working thermodynamic model has not been completed; when it is done, the data collected from the HACS will be more than sufficient to compare theoretical best-case scenarios. Lastly, comparisons between conventional

HVAC system performances and costs can be carried out, further illustrating the advantages of the HACS system.

3:6 EXPERIMENTAL UNCERTAINTY

Running the tests described above on the prototype HACS is an excellent way to demonstrate the system's advantages. The data collected from running the tests can provide numerical proof of the potential abilities of the prototype system. On the other hand, in order to assess whether the data collected are a valid demonstration of the HACS capabilities, an uncertainty assessment on the experimental data is required.

First, it is important to point out that the error cannot be calculated exactly unless the true value of the quantity being measured is known. Within our prototype system there are bias "B_x" and precision "P_x" uncertainties [18]. The total uncertainty "U_x" is defined as [18]:

$$U_x = \left(B_x^2 + P_x^2\right)^{\frac{1}{2}} \tag{7}$$

The total uncertainty is the square root of the sum of the squared bias and precision uncertainties. The precision uncertainties are defined as [18]:

$$P_x = \frac{tS_x}{\sqrt{n}} \tag{8}$$

Where t is the t-statistic, S_x is the sample standard deviation, and n is the sample size [18]. In most cases the bias uncertainties are user-estimated [18].

All the instrumentation for collecting data from the HACS has been calibrated for its specific use. Thermocouples were calibrated within a range of temperatures using a precise hot water bath paired with an ice bath. The hot water bath allowed for the user to digitally set the device to heat the water to a specific temperature within the range from 20 ^{o}C to 100 ^{o}C. The error presented with this calibration derives from the error within the temperature sensor for the hot water bath. The hot water bath had a name plate error of ±0.1 ^{o}C. Thermocouple calibration was performed starting with the thermocouples placed in the ice bath, representing 0^{o}C. The temperature output of the thermocouples was recorded at this point. Next, the thermocouples were transferred to the hot water bath. The hot water bath was set initially at 20 ^{o}C and was increased in increments of 5 ^{o}C until 100 ^{o}C was achieved. The voltage readouts from the thermocouples were recorded during each 5^{o}C step. The resulting calibration curve had an accuracy of ± 0.1 ^{o}C for the temperatures ranging from 20 ^{o}C to 99 ^{o}C, and the 0 ^{o}C and 100 ^{o}C points are exact known temperatures, thus accompanied with no error. The calibration curve that was attained can be viewed in Figure 3.4.

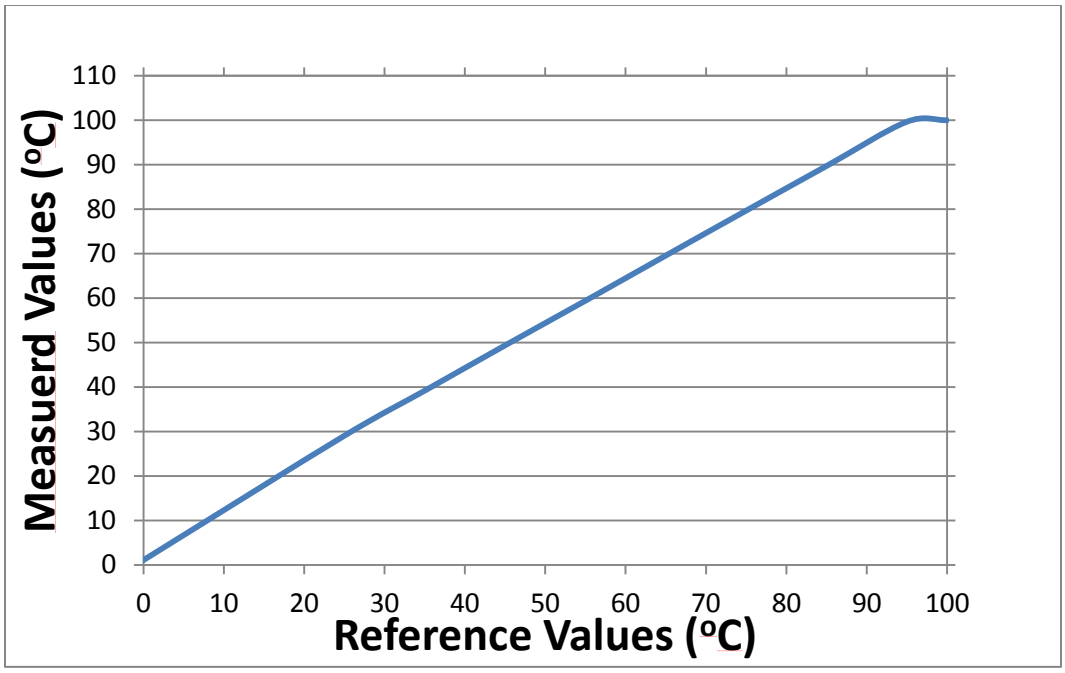

Figure 3.4 Thermocouple calibration curve

The calibration curve that was produced from this test was then uploaded into a LabVIEW file and used as a reference for the thermocouple readings. Looking at the calibration curve in figure (3.4) it is important to note the linear in continuity from just above 95 ^{o}C to 100^{o}C. This could be a result of the inaccuracy of the hot water bath temperature sensor. The produced calibration curve allowed for accurate thermocouple readings, with the main source of error coming from the ± 0.1 ^{o}C accuracy of the hot water bath.

The pressure transducers that were installed within the refrigerant inlet and outlet lines from the compressor have a readout range of 0-300 psig. The listed specifications from the manual on the product showed an accuracy of ±0.25%[19]. Thus, any pressure measurements taken from our system were within an uncertainty range of ±0.25%.

There were two rotameters installed, one inserted within the refrigerant liquid line from the compressor, and the other inserted on the outlet side of the glycol air handler. The rotameter for the refrigerant line was professionally calibrated by King Instruments for use with refrigerant. The rotameter was shipped with a known accuracy of ±2.0% of full scale flow. On the glycol side, the rotameter purchased was a King Instruments 72 series rotameter specifically made for water. The glycol rotameter was meant for water and is being used in a water/glycol solution with the ratio of 35:1.5 water to glycol. Thus, it is safe to assume that the fluid going through the glycol rotameter is 95.89% water. The claimed accuracy of the rotameter was between ±3% of full scale [20]. The major error introduced with the rotameters is the analog output that they display. The biggest source of error is in the visual reading of the rotameter.

In order to read the voltage supplied either from the grid or PV modules, a voltage divider circuit was installed across the outlet that the DC controller board plugs into. The voltage divider circuit uses a pair of resistors (R_1 and R_2) to divide an input voltage V_1 into a smaller output voltage V_2 [18]. The output voltage measured across R_2 is then [18]:

$$V_2 = \frac{R_2}{R_1+R_2} V_1 \tag{9}$$

In the HACS system, the minimum voltage supplied is 130V coming from the grid. The maximum voltage supply is 165V, supplied from the PV modules. Thus the voltage divider was designed to output a volt reading

for a range of 0-200 V. The chosen R_1 and R_2 values were 195 kΩ and 5 kΩ, based on a 200 V_1 input. This would supply a voltage output reading range of 0-5 V with 0 equaling true 0 V and 5 V equaling 200 V.

There is one major source or error within reading the voltage sensors. The resistors used to construct the voltage divider are not 100% accurate. They are color-coded by the manufacturer for both size and accuracy. The resistors used in the HACS all had a gold band, representing an accuracy of ±5% [19]. R_1 and R_2 were constructed using multiple resistors, and table 3.6 represents their makeup.

Table 3.6 R_1 and R_2 resistor compilation

R_1 = 195KΩ	**R_2 = 5kΩ**
9x10kΩ	2x2.2kΩ
2x2.2kΩ	2x300Ω
2x300Ω	
1x100kΩ	

When measuring the resistance with a digital meter, the actual resistance of R_1 and R_2 was 186 kΩ and 491 Ω respectively. Both of the actual recorded resistances of R_1 and R_2 were taken with a digital multimeter that was accurate up to ±0.5 Ω [21]. R_1 was within 95.38% of the marked resistor value and R_2 was within 98.2%. After acquiring the actual resistance of R_1 and R_2, the curve to calculate the correct output voltage was formed, which was accurate up to a half-digit.

In order to measure the current supplied from either the grid or PV modules, shunt resistors were installed in series with each power source

within the power selector box, as displayed in Figure 1.4. The two shunt resistors relate a specific millivolt output to a corresponding current. The shunt resistor for the PV modules had a 0-50 mV output that corresponded to 0-16 A current. The grid power shunt resistor consisted of a 0-50 mV output which was directly related to a 0-20 A current. Both of the shunt resistors have a claimed accuracy of ±0.25%.

The final source of error in data collection stems from the data acquisition device that interfaces with the LabVIEW computer program. The data acquisition device is a SCB-100. The device was specifically built to read sensors with a voltage output [22]. Figure 3.5 displays the SCB-100.

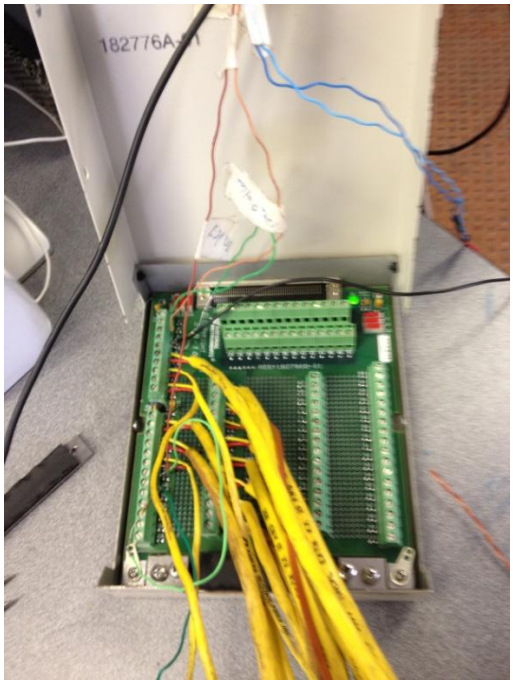

Figure 3.5 SCB-100

As shown in Figure 3.5, it is clear that there are many sensors plugged into one single device. In order to keep the electrical noise to a minimum, all the floating signal sources such as the thermocouples were tied to analog ground with a 200 Ω resistor. This provided a return path for the instrumentation bias currents. The specific error limitations of the SCB-100 are minimal. For thermocouple use, the device has an error of ±0.5 ^{o}C, which was avoided due to the thermocouple calibration. Using the SCB-100 for measuring the pressures, currents, and voltages the specified source of error is due to gain, and results in a ±0.08% uncertainty [22]. The added error from the sensor data acquisition device is very minimal, but does create cumulative error on top of the initial installed instrumentation error.

The major calculations performed from the data collected from the system include cooling power of both air handlers, coefficient of performance (COP), and the overall electrical efficiency of the system. For the calculations discussed, the equations involved are (1) through (6). After sample data on the HACS has been collected, the uncertainty variables that have been discussed can be inserted into Equations 7 and 8, and the total uncertainty may be calculated. Table 3.7 lists the estimated uncertainties of the calculations.

Table 3.7 Uncertainties within calculations

Calculation	**Instrumentation**	**Estimated Uncertainty**
$COP_{refrigerant\ loop}$	current, voltage, thermocouple, DAQ, rotameter	±2.0%
$COP_{thermal\ storage\ loop}$	current, voltage, thermocouple, DAQ, rotameter	±3.0%
COP_{HACS}	current, voltage, thermocouple, DAQ, rotameters	±3.6%
Cooling power of glycol air handler	thermocouple, DAQ, rotameter	±3.0%
Cooling power of refrigerant air handler	thermocouple, DAQ, rotameter	±2.0%

Looking at table 3.7, the expected uncertainties do not add up to very much. However, it is important to note that these calculations can be misleading. Each calculation involves the uncertainty of a rotameter. Even though the stated uncertainties of the rotameter are very small, human error can be introduced during the reading process. Even though this added human error is not accounted for in the calculations, it should not go unnoticed. A way of minimizing the human error would be to have the same person always read the rotameters, always following the same method of documentation.

Chapter 4: RESULTS AND DISCUSSION

4:1 TECHNICAL DIFFICULTIES

At the present time, the prototype HACS system is out of commission. Due to the fact that everyone working on this project was fairly new to heating ventilation and air conditioning systems, there were many obstacles that came into play. Since this is the first time that this type of system has been built, many unforeseen roadblocks are to be expected. For example, the DC compressor purchased for the project had never been run on such a big system involving two evaporators. This turned out to be a major problem, because the oil contained within the compressor upon installation was not enough for such a large system. With two evaporators, the oil was unable to cycle through the refrigerant lines and smoothly return to the compressor. Without oil cycling back to the compressor to keep the bearings greased, the compressor lifetime was severely shortened. Due to the compressor's short lifetime, only minimal data on the system could be collected.

4:2 EXPERIMENTAL RESULTS AND DISCUSSION

None of the outlined tests discussed in chapter 3 could be performed fully. On March 8 2012, the system was successfully turned on in order to see if ice could be produced. We were able to leave the system on for about a 5-hour time period. The system was turned off in order to avoid complete freezing and damaging the evaporative coils, due to glycol

not being added to the thermal storage yet. During this charge up time, no data could be collected due to faults in the LabVIEW program. After the program was fixed, on the following day a simple test was performed to view the cooling power of the thermal storage, along with its longevity. The thermal storage was pumped through its corresponding air handler, while the rest of the prototype system was turned off. The only components requiring electrical power were the glycol thermal storage pump (35 W), and air handler (200 W). The ice thermal storage was deemed ¼ of the way frozen from the top down when the test was started. The system was allowed to run overnight and turned off in the morning after the ice had completely melted. The glycol flow rate was constant and read $1.51*10^{-4}$ m^3 s^{-1} or 2.4 gallons per minute. It is important to note that the air handler turned off for a 15-minute period due to the temperature setting on the thermostat being met. In order to prevent this from happening again, and sustain continuous cooling with the glycol air handler running, the thermostat was turned down to its lowest temperature setting of 8.3 ^{o}C or 47 ^{o}F. Figure 4.1 shows the room temperature during the time the test was performed.

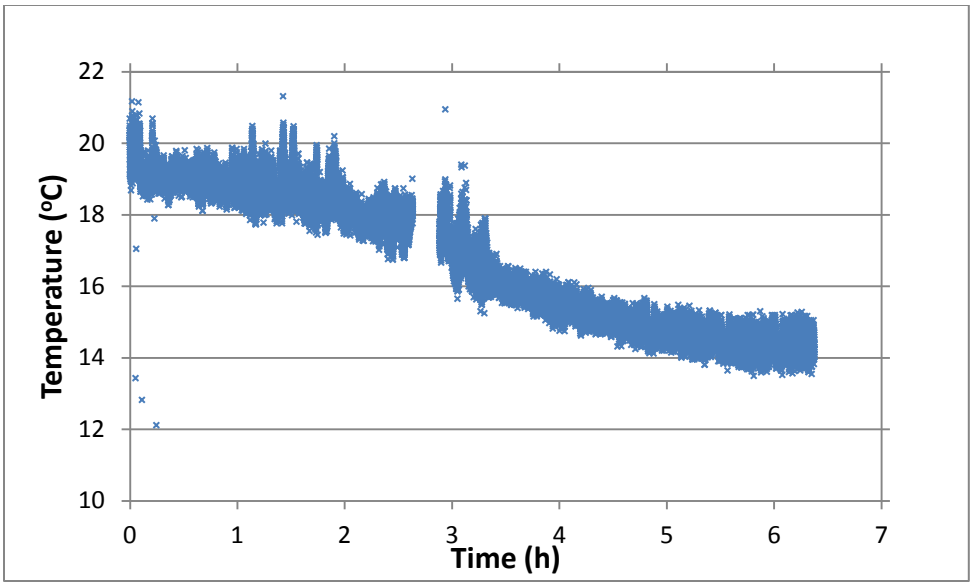

Figure 4.1 Room temperature over time

In order to acquire a good understanding of the cooling power supplied during this test, comparisons needed to be made between the temperatures within the lab versus the outdoor ambient temperature. The test was run starting at 5pm on March 8, 2012. Table 4.1 shows the outdoor ambient temperatures during the 6-hour time period of the test run [23].

Table 4.1 Recorded ambient temperatures on 3/8/2012 [23]

Time	Recorded Temperature ^{o}C
4:51pm	21.7
5:51pm	21.7
6:51pm	21.1
7:51pm	20.0
8:51pm	18.2
9:51pm	19.4

It is important to note that the lab with which the HACS is located is a poorly insulated space on the roof of a building. Taking that into

consideration while comparing the temperatures in table 4.1 with Figure 4.1, it is clear that the thermal storage was able to provide a considerable cooling load.

Figures 4.2 and 4.3 show the cooling power over time of the glycol air handler.

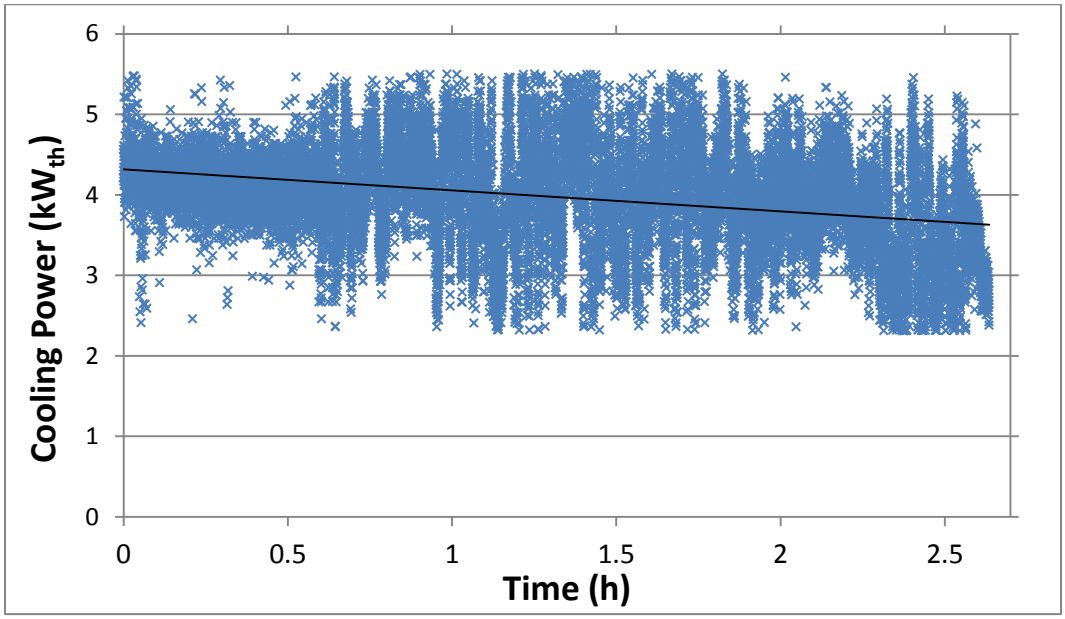

Figure 4.2 First section of the cooling power over time of the thermal storage

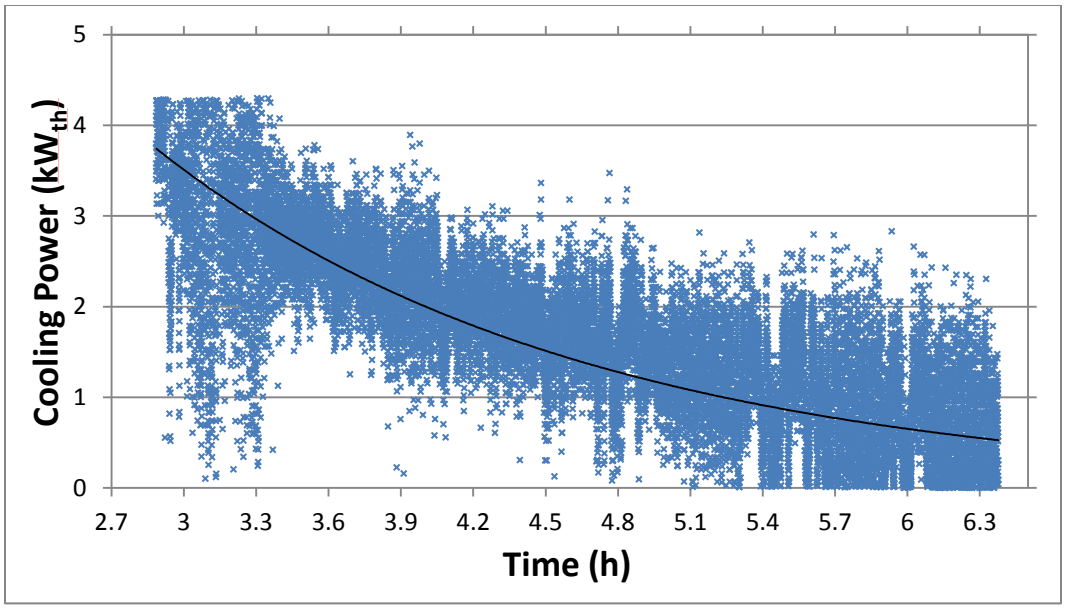

Figure 4.3 Cooling power after 15 minute shut off

The cooling power in Figures 4.2 and 4.3 was calculated using Equation 5 from Chapter 3 along with the density and specific heat of water. From Figure 4.1 it is clear that the glycol air handler started out producing just over 4.5 kW_{th} of cooling power. This was above our requirement of producing 3.5 $kW_{th,}$ or 1 ton of cooling power with the glycol air handler.

Figure 4.2 shows that above 3.5 kW_{th} of cooling was able to be sustained for 2 hours and 38 minutes, which is when the glycol air handler shut down. The 15-minute time period when the glycol air handler shut off is very interesting to analyze. The start of the plot in Figure 4.3 shows the cooling power of the thermal storage to recharge back to almost 4 kW_{th}. This recharge may be explained by the returning water from the glycol air handler having a greater period of time to cool back down

before it entered the pump to return to the glycol air handler. The cooling power of the glycol air handler in Figure 4.3 stayed above or equal to 3.5 kW_{th} or 1 ton until the 3 hour 18 minute mark of the test. It is also important to note the exponential decay in Figure 4.3. The observation of the exponential decay of the cooling power is a great example of the thermal temperature time constant.

Subtracting 15 minutes from the time of 3.2 hours, it can be estimated that the ice thermal storage supplied ≥3.5 kW_{th} of cooling for almost 3 full hours. The cooling power of the glycol air handler became negligible after a total run time of 6 hours and 22 minutes. This initial test is very significant in that it proves the ability of the system to store PV power for later efficient use. Correspondingly, if one were to say that a ¼ frozen freezer equaled approximately 3 hours of effective cooling, one could extrapolate the numbers and assume that if the freezer was ¾ frozen from the top, the cooling power of the glycol air handler could be ≥3.5 kW_{th} for approximately 9 hours.

It is also important to note the temperatures within the thermal storage and understand their relevance with respect to the cooling power of the glycol air handler. The average temperature of the thermal storage and the cooling power throughout the testing period is shown in Figure 4.4.

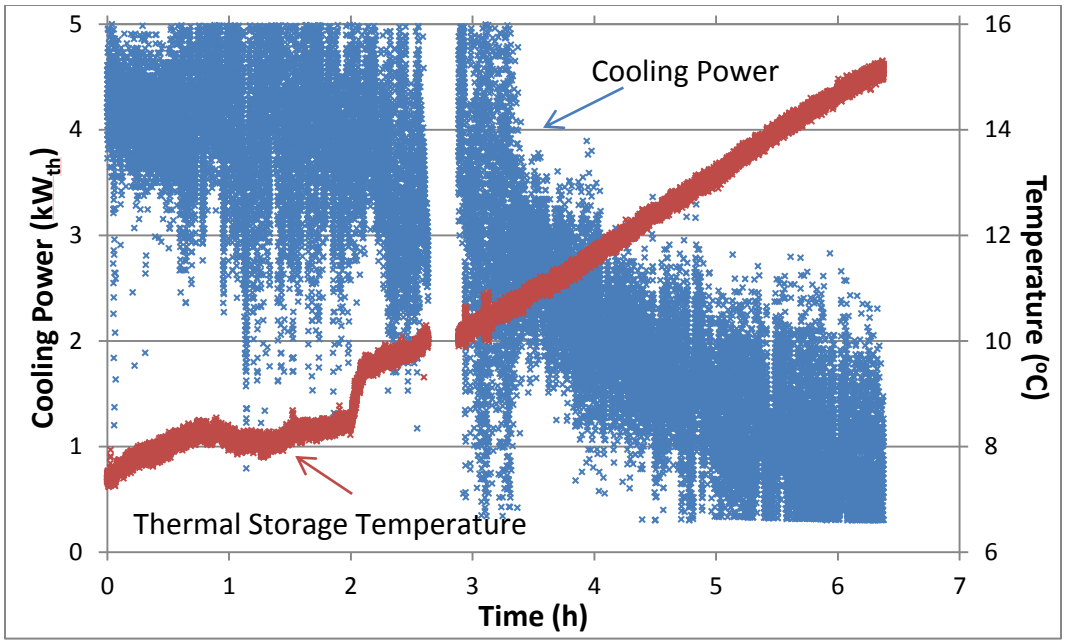

Figure 4.4 Temperature of thermal storage vs. cooling power

Figure 4.4 demonstrates that when the average temperature of the thermal storage rises above 11°C, there is not enough energy within the thermal storage to provide the temperature gradients across the glycol air handler so that the cooling power can be at 3.5 kW_{th}. Therefore, it is safe to conclude that the average temperature within the thermal storage has to be ≤11°C.

Another interesting observation concerning the temperatures within the thermal storage concerns the gradients of temperatures within the thermal storage. Placed within the thermal storage were 9 thermocouples. There were two in each corner, (one at the top and one at the bottom) and one in the center of the thermal storage. Table 4.2 shows the acronyms that describe the placement of the thermocouples.

Table 4.2 Positional acronyms

Position	Acronym
Thermal Storage	TS
Center	C
Front Right Top	FRT
Front Right Bottom	FRB
Front Left Top	FLT
Front Let Bottom	FLB
Back Left Top	BLT
Back Left Bottom	BLB
Back Right Top	BRT
Back Right Bottom	BRB

Figures 4.5-4.13 display the different temperatures that each thermocouple within the thermal storage displayed during the testing period.

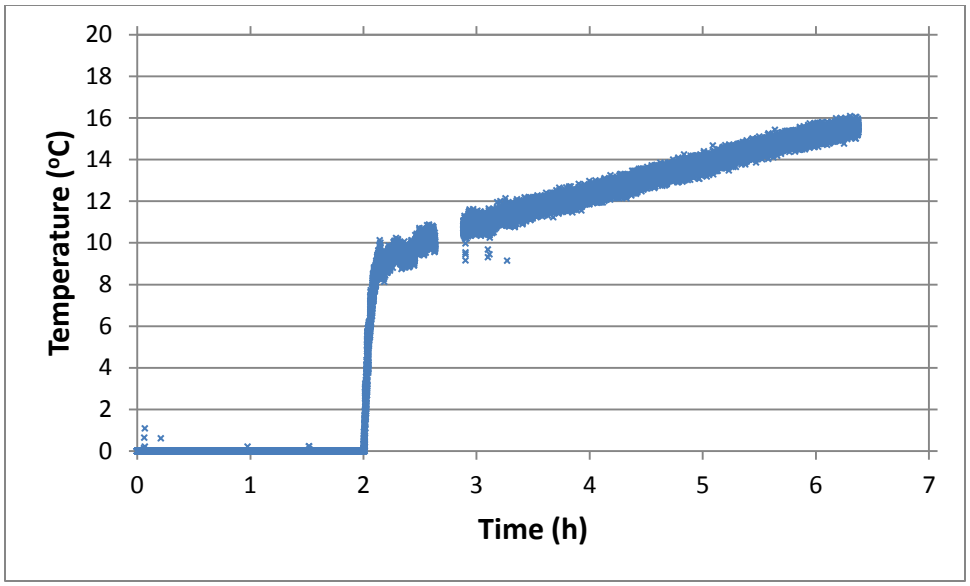

Figure 4.5 Thermal storage: center

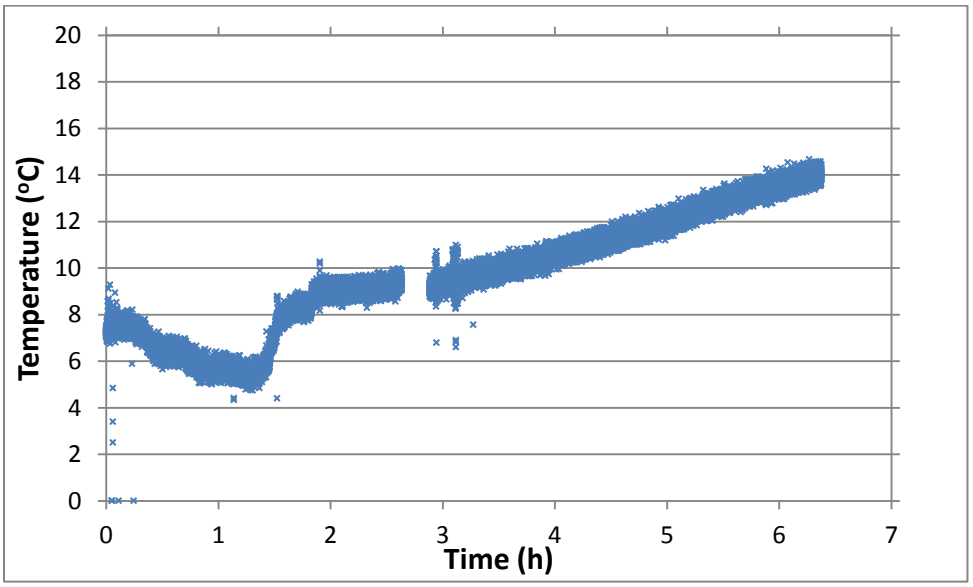

Figure 4.6 Thermal storage: front, right, top

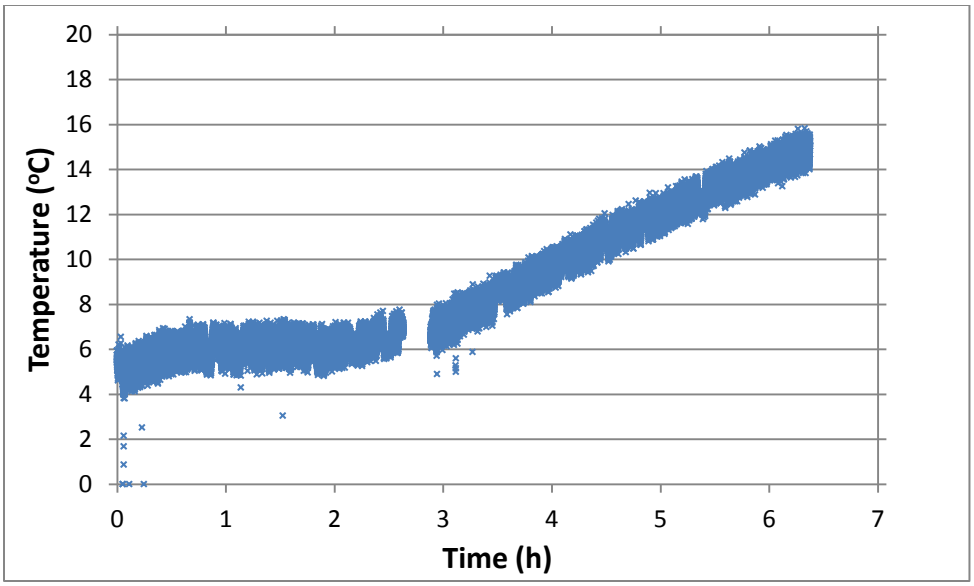

Figure 4.7 Thermal storage: front, right, bottom

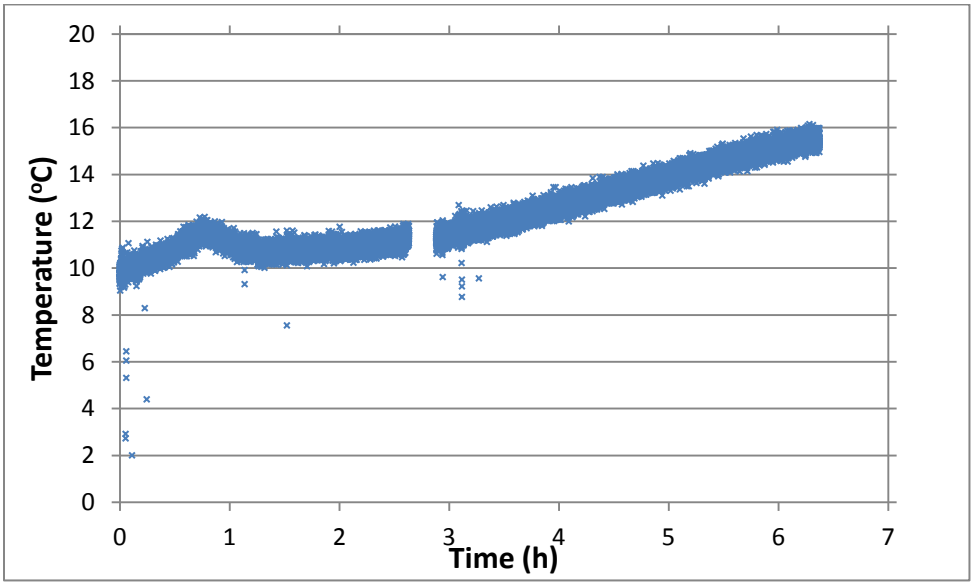

Figure 4.8 Thermal storage: front, left, top

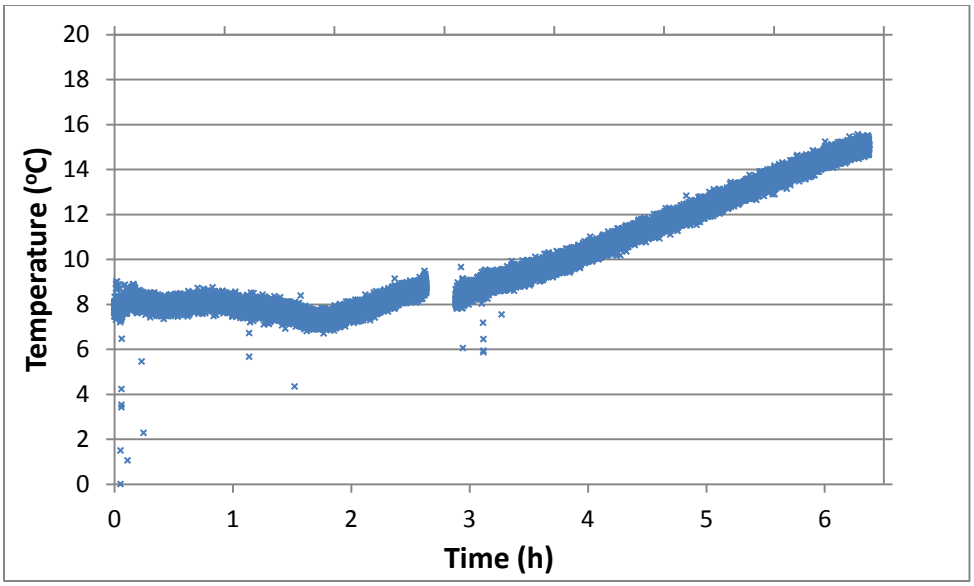

Figure 4.9 Thermal storage: front, left, bottom

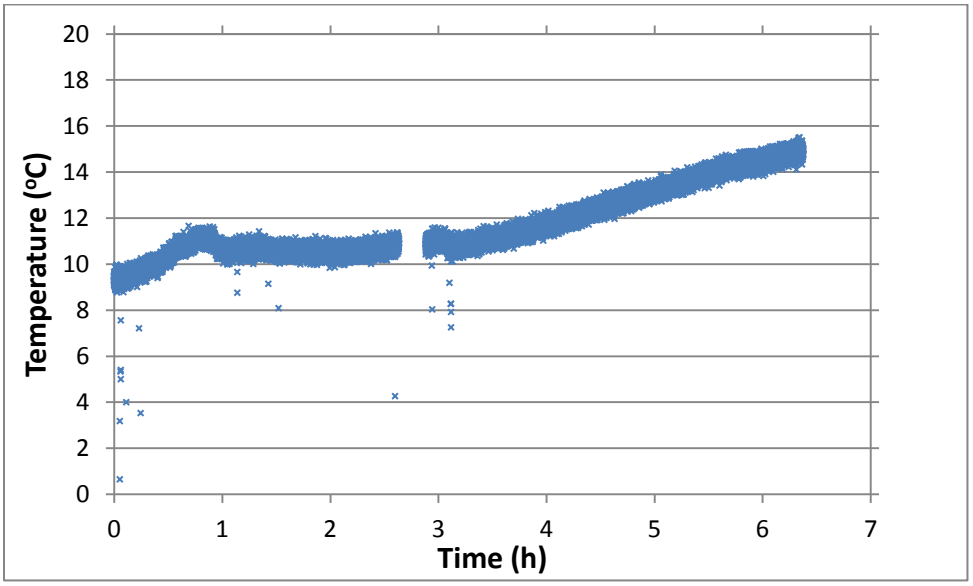

Figure 4.10 Thermal storage: back, left, top

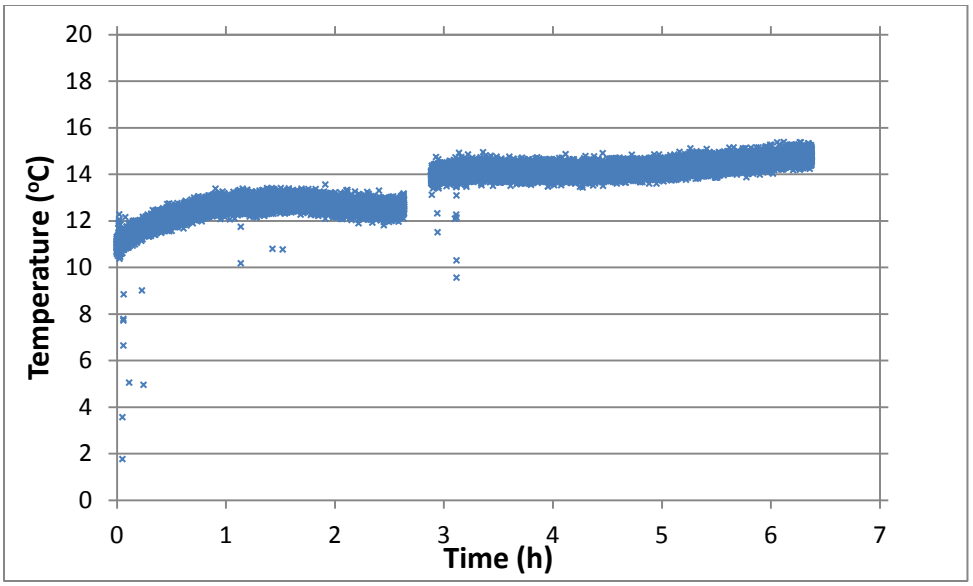

Figure 4.11 Thermal storage: back, left, bottom

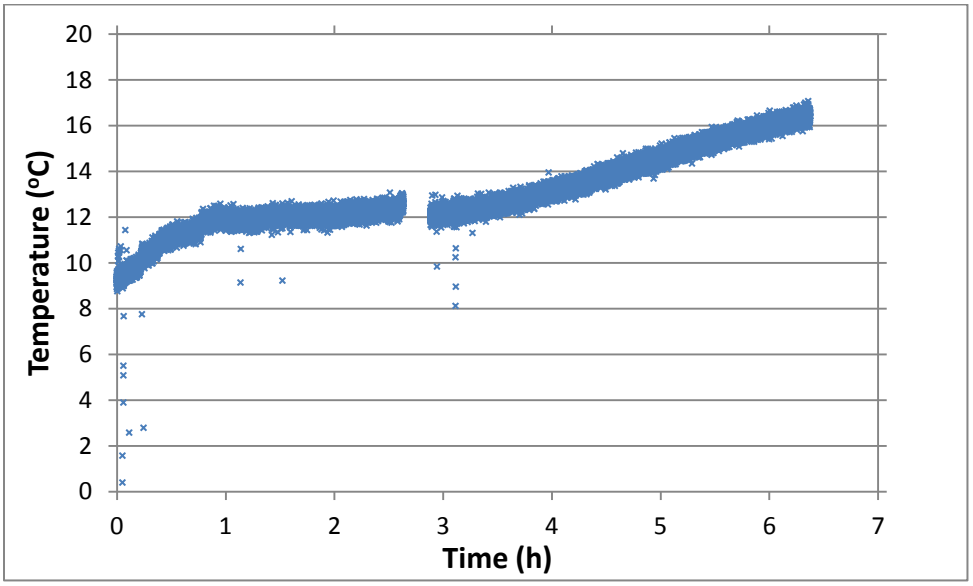

Figure 4.12 Thermal storage: back, right, top

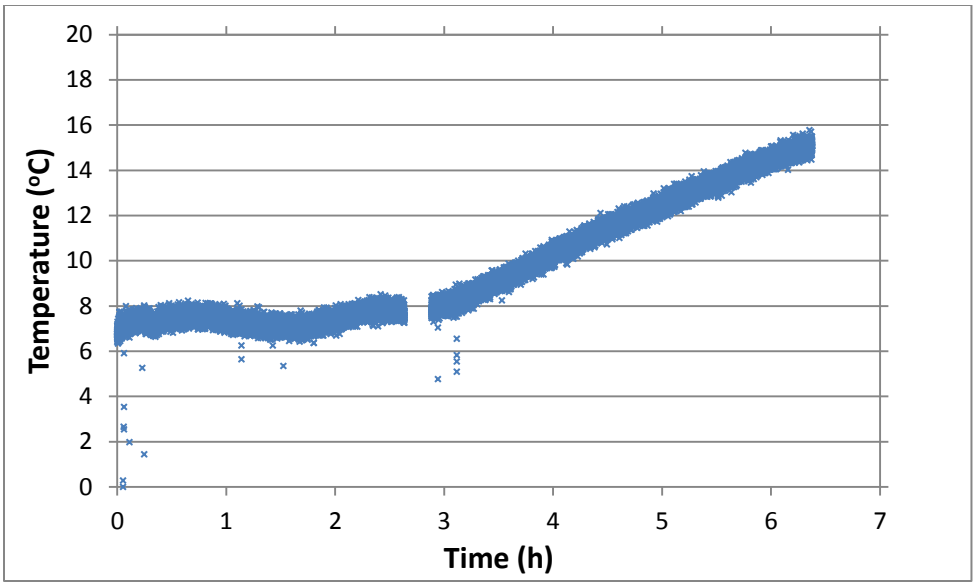

Figure 4.13 Thermal storage: back, right, bottom

Looking at Figures 4.5-4.13, it is interesting to see that the thermal storage holds its temperatures fairly well until the 3 hour mark. It is also important to note the 15 minute gap that occurs in the test, easily noticeable in each figure.

The final analysis on this test can be done by looking at the temperature difference across the glycol air handler. Figure 4.14 shows the temperatures across the glycol air handler.

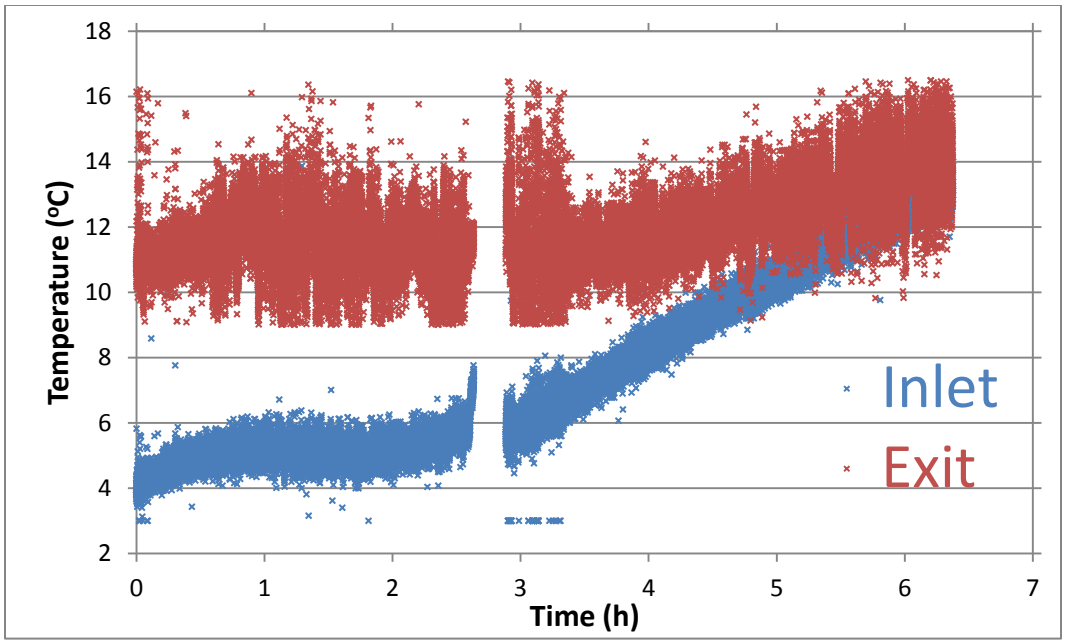

Figure 4.14 Temperature across glycol air handler

As seen in Figure 4.14, the temperature gradient across the inlet and exit to the glycol air handler needs to be a minimum of 5 ^{o}C in order to obtain 3.5 kW_{th} of cooling. With this required temperature gradient in mind, the design of future thermal storage and air handler design prototypes can be optimized.

The time period from which the thermal storage would most likely have to be used is from 12pm-8pm daily, when the electricity rates are the highest. It is important to note that the PV modules can run the whole system until there is insufficient solar radiation. The DC compressor that is installed in the HACS system can run off of a minimum voltage and power of 90V and 855W. The PV modules were measured at 10am, 12pm and 5pm on May 21 2012. It is important to note the maximum working

voltage that the PV modules can supply is 165V. Table 4.3 shows the recorded voltages at the specified times.

Table 4.3 Recorded voltages

Time of Day	Voltage (V)
10am	150
12pm	162
5pm	156

The voltages in table 4.3 were taken using a heating element as a resistive load across the PV modules. The measured resistance of the heating element was 18.5Ω. Using this information the power output of the PV modules was calculated and is shown in table 4.4.

Table 4.4 Calculated power output of the solar modules

Time of day	Voltage (V)	Power (W)
10am	150	1248
12pm	162	1441
5pm	156	1315

The calculated power outputs of the solar modules in table 4.4, is almost 1000W less than their nameplate ability solar modules (2300W). This may be due to the solar panels being dirty and thorough cleaning would solve this problem. As stated previously, the minimum power to needed run the DC compressor is 855W. The listed voltage measurements

and power calculations are well above the minimums required to run the DC compressor, showing that the PV modules could run the DC compressor for approximately 7 hours per day.

It is also necessary to calculate the angle of the sun with respect to the horizon during the previously specified times. Table 4.5 shows the calculated solar elevation angle of the sun corresponding to the times that the voltage measurements were taken [24].

Table 4.5 Solar elevation angle

Time	**Solar Elevation Angle (°)**
10am	40.89
12pm	65.20
5pm	42.85

Analyzing Table 4.5, it can be shown that the sun needs to be at a minimum elevation angle of 40.89 degrees in order for there to be enough solar radiation striking the solar modules to power the HACS. Therefore, the solar panels could power the HACS from 10am till 5:30pm (7.5 total hours) on the date of May 21 2012. With this assumption, and looking at data of the solar elevation angle with respect to time and day of the year, the HACS could be powered by the solar panels on an average of 10am – 5pm during the months of May through August [23], [24]. If the solar modules can power the system until 5pm daily, the thermal storage may

only be needed for the peak energy rate hours of 5pm-8pm. Another important point is that cooling may be needed prior and beyond the dates of May through August. Looking at the monthly average temperatures of April (22.7 ^{o}C) and September (31.1 ^{o}C), it could be noted that cooling may be needed at those times, but not at such a high demand as the time from May through August [23]. Lastly, it must be noted that as the solar radiation decreases, during the month of September for example, the thermal storage will be needed to run for longer periods of time. Thus it is important to ensure adequate auxiliary thermal storage for days when there is minimal solar radiation.

4:3 CHARGING THE THERMAL STORAGE

Understanding the amount of time it takes to charge the thermal storage is a very relevant topic when discussing the abilities of the HACS. In order to know the time required to charge the thermal storage, the amount of energy required needs to be calculated. The amount of energy required to charge the thermal storage was calculated for two specific situations: pure water, and a 5% glycol solution. In order to calculate the energy required to charge the thermal storage, the mass of liquid, Cryogel balls, water bottles and oil containers needed to be calculated. Tables 4.6 and 4.7 show the distributed calculated masses for water and the 5% glycol solutions.

Table 4.6 Pure water thermal storage

Substance	Amount	Mass (kg)
Water	40 gallons	151.00
Cryogel balls	8 cubic feet	79.46
12 oz water bottles	30	10.65
1 quart oil containers	25	23.66
total mass		264.77

Table 4.7 5% glycol solution thermal storage

Substance	information	mass kg
Water	38 gallons	143.8
Cryogel balls	8 cubic feet	79.46
12 oz water bottles	30	10.65
1 quart oil containers	25	23.66
glycol	2 gallons	18.44
total mass		276.01

Using the basic equations of heat transfer, the energy required to charge the thermal storage to -1^{o}C was calculated and is displayed in Table 4.8 [25].

Table 4.8 Energy required to charge the thermal storage

Solution	Q (kJ)
Water	110337
5% Glycol	114313

The DC compressor can operate at a 3.5 kW_{th} h^{-1} capacity as long as the evaporator temperature is not below -12^{o}C. The time to charge the thermal storage could be modeled by dividing the energy required to charge the thermal storage by the energy supplied by the compressor.

Table 4.9 shows the estimated times to charge the water and 5% glycol solution thermal storage.

Table 4.9 Charge times

Solution	Charge Time (h)
Water	8.75
5% Glycol	9.07

Table 4.8 shows that the estimated charge times for both solutions are only differentiated by 18 minutes. This difference in time may be explained by the small differences in specific heats of the two solutions. Charging the thermal storage could be done overnight when the cost of power is least expensive. It is important to note that these charge times are only an estimate, and require verification by experiment.

4:4 VALIDITY OF RESULTS

With the initial data collected, it is clear from looking at Figures 4.2 and 4.3 that there is a lot of noise within the data. After much troubleshooting, it was concluded that the numerous thermocouples all plugged into one data acquisition device were the source of the noise. The problem was that due to having so many thermocouples entering one data acquisition device, the small currents within each thermocouple wire were inducing noise into neighboring thermocouples. Through extensive reconfiguring and problem solving, each thermocouple was tied to analog ground through an 200 Ω resistor. This helped with the noise issues, and

allowed the only error within the temperature data to be a direct result of the limits of the data acquisition device. The rotameter that was inserted into the glycol thermal storage lines was meant for water, thus it is already calibrated to have an accuracy of ±3.0%. The main error from the rotameter then is the visual reading of it. Even though there is little to no data yet on the system, the error that may be introduced when taking measurements come from the refrigerant rotameter and the pressure transducers inserted within the vapor and liquid refrigerant lines. The refrigerant rotameter was calibrated upon purchase for refrigerant, and thus is stated to be accurate between ±2.0% at full length. The pressure transducers are very simple devices that introduce minimal error. Even though they are not calibrated for R134a, they still read the line pressures and those can be compared to an R134a conversion chart for accuracy. The data collected is significant, and further testing should be able to demonstrate the abilities of the HACS very well.

Chapter 5: DC VS. AC POWERED SYSTEM

5:1 COST COMPARISON

The original direct current "DC" powered system posed many different advantages and disadvantages. The DC system was proposed in order to accommodate the need for forward operating bases to achieve a smaller power requirement, thus decreasing the size of the resupply chains that travel to the forward operating bases, and to thus minimize risk to soldiers. The initial system was conceived for locations with minimal or no grid connectivity. A DC system was optimal for these types of applications, because there would be minimal power losses from the PV modules to the DC compressor due to the fact that no inverter was needed.

As of late May 2012, planning and construction of a new second stage prototype has been underway. The new system will be an alternating current system (AC), with an AC compressor. As the research on hybrid air conditioning systems has progressed, other uses for the HACS have surfaced. From the perspective current issues such as global climate change, the residential and commercial market for a HACS system has become very intriguing. In order to understand which system best fits the residential and commercial industry, analysis of the comparative costs and advantages/disadvantages between DC and AC powered system was performed. Regarding the cost analysis, it was discovered that the PV

modules cost was $293/module, or $2,093.00 for a total of 10 modules [28]. The cost analysis between DC and two different AC systems is shown in Tables 5.1-5.3.

Table 5.1 DC system prices [28], [29]

DC System Parts	Manufacturer / Part No.	Price
DC Compressor 1 ton (R134a)	Masterflux SIERRA05-0982Y3	$ 675.00
Motor Controller	Masterflux 025F0062-01	$ 819.00
2 Thermostats	LUX TX500E	$ 100.00
Thermal Storage Temperature Controller	Omron E5AX	$ 200.00
HVAC air handler	Air Con ACN1318HPCCOEV	$ -
Glycol Air handler	LG LSN122HE	$ 440.00
Variac	STACO Energy Products	$ 222.00
2 Solenoid Valves	Parker 6B05	$ 250.00
Unit Price (Excludes PV modules)		$2,706.00
Total Unit Price		**$5,636.00**

Table 5.2 AC system one [30], [31] *Included with compressor purchase

AC System Parts	Manufacturer / Part No.	Price
AC Compressor 1 ton (R410a)	Ramsond R37GW2	$ 830.00
Inverter	SMA Sunny Boy 700-US	$1,038.00
2 Thermostats	LUX TX500E	$ 100.00
Thermal Storage Temperature Controller	Omron E5AX	$ 200.00
HVAC air handler*	Ramsond	$ -
Glycol Air handler	Ramsond replacement coil 195	$ 195.00
2 Solenoid Valves	Parker 6B05	$ 250.00
Unit Price (Excludes PV modules)		$ 2,613.00
Total Unit Price		**$5,543.00**

Figure 5.3 AC system with variable speed compressor [28], [31], [32]

AC System With Variable Speed Compressor	Manufacturer / Part No.	Price
Variable AC Compressor 1 ton (R410a)	Mitsubishi MSZ/MUZFE09NA	$ 1,516.00
2 Thermostats	LUX TX500E	$ 100.00
Thermal Storage Temperature Controller	Omron E5AX	$ 200.00
HVAC air handler*	Omron E5AX	$ -
Glycol Air handler	LG LSN122HE	$ 440.00
2 Solenoid Valves	Parker 6B05	$ 250.00
Inverter	SMA Sunny Boy 700-US	$ 1,038.00
Unit Price (Excludes PV modules)		$3,544.00
Total Unit Price		**$6,474.00**

It is clear that the price of the AC system in table 5.2 is a little less than that of a DC system. The original HACS system was built as a DC system in order to make it usable in forward operating basis with no grid connection. On the other hand, if one were to install the original DC HACS for residential and commercial use, and wanted to feed the excess PV power back into the grid, an inverter would need to be purchased. The added cost of an inverter, such as the one in table 5.2, for a DC system would increase the capital cost by another $1,038.00, making the DC system even less cost-effective.

In order to avoid the cost of an inverter in the DC powered system, alternative uses for the excess PV power were discussed. A DC specific power outlet could be installed within the residency and used to power multiple contraptions, such as those listed in table 5.4.

Table 5.4 Excess PV power options for DC powered system

Electric car charging station
Hot water heater
Electronic accessory charging port
Electric stove – oven heating element
Lighting

The ideas presented in table 5.4 could offer great advantages. In order to implement any of these excess PV power options, a DC specific outlet would need to be installed within the house, further increasing the parts list and capital cost of the DC powered system.

The comparison in price of an AC powered HVAC system being less expensive versus a HVAC system with a DC compressor is also due to the ubiquity of the AC powered system. Because AC powered HVAC systems are highly mass-produced, their costs are much lower, even to the degree that adding an inverter to the initial cost of the system still keeps it more cost effective than a DC powered system.

Installing an AC powered system may also be simpler due to the fact the HVAC manufacturers are more familiar with AC powered systems than with DC powered systems. The ease at which the excess PV power can be used is also very intriguing. Through an inverter, the excess PV power can be fed directly back into the grid, allowing users to further increase their cost savings on electricity. Alternatively, the excess PV

power can be supplied to any power outlet within the residency without any specific added installations being performed.

5:2 PERFORMANCE COMPARISONS

From a thermal standpoint, both the DC and AC powered systems should perform similarly. The thermal storage should charge and discharge in comparable intervals of time. The conventional air handlers will have similar cooling powers and will draw analogous electrical power. Addressing the electrical performance of each system, however, allows the main differences between the systems to become evident.

The DC powered system will have minimal power losses from the PV modules to the DC compressor. This will allow for maximum use of the power produced from the PV modules to run the system. Over long periods of time, the small amount of extra solar radiation able to be used for powering the system may have a cumulative effect on electricity savings. The only problem with the DC powered system is that difficulties are encountered when one wants to figure out what to do with excess PV power. As of now, the original HACS does not supply excess PV power to the grid, thus missing its potential to vastly decrease the meter reading. Lastly, this DC powered system can easily be implemented for off-grid use because of its relative simplicity; everything is DC powered and fewer components are required to build the system.

The AC powered system's main fault is the electrical losses through the inverter. The inverter that is being installed has a maximum efficiency of 93.3% and a California Energy Commission (CEC) efficiency of 91.5% [31]. This 6.7-8.5% loss can add up quantitatively over long periods of time, and could result in not only electrical losses but long term economic losses. Because of this power loss through the inverter, the PV modules will not be able to run the system for equal amounts of time during each day, when compared to the DC powered system. On the other hand, the ease of installation along with the ability to casually feed power back into the grid will allow for large cost savings. All in all, the electrical advantages and disadvantages between the two systems are very clear. In order to make the DC system have the ability to perform similarly to the AC powered system, i.e., to feed excess power back to the grid, the capital cost will increase. Even with the AC powered system's initial electrical losses, it is clear the system is the more economical option, and therefore represents a better model for residential and commercial use. The pros and cons of the AC and DC powered systems can be observed in Table 5.5.

Table 5.5 Pros and cons of AC and DC powered systems

AC Powered System		DC Powered System	
Pros	**Cons**	**Pros**	**Cons**
Ability to feed excess PV power back to the grid	Electrical losses through the inverter	Minimal electrical losses	Price
Price	Not easily ready for off grid use	Ready for off grid applications	Needs added inverter for grid tied applications
Ease of installation			What to do with excess DC power

5:3 COEFFICIENT OF PERFORMANCE COMPARISONS

Coefficient of performance (COP) is the best indicator of the operating efficiency of a heat pump. As of now, there is not enough information to get the exact COP of the HACS using the equations discussed in Chapter 3. An estimated COP of the HACS can be obtained by performing operational research on the compressor performance, and making some basic operating assumptions. Since data on the HACS was collected for only a few days, the estimated COP will then correspond to the day the PV modules were tested (May 21 2012). The factors that were researched and assumed in order to estimate the COP of the HACS are outlined in Tables 5.6 and 5.7 [27].

Table 5.6 Researched assumptions for DC powered system

Researched Assumptions for DC system	Power Input
cooling power of HVAC air handler	3.5 kW
Thermal storage evaporator cooling power	3.5 kW
Cooling power of glycol air handler	3.5 kW
PV power supplied	1.150 kW
Grid Power supplied	1.150 kW
Mass flow of the refrigerant	62.79 kg/hour
glycol pump power	35 W
glycol air handler power	200 W
HVAC air handler power	150 W
condenser fan power	150 W

Table 5.7 Researched assumptions for AC powered system *powered from the compressor [30]

Researched Assumptions for AC system	Power Input
cooling power of HVAC air handler	3.5 kW
Thermal storage evaporator cooling power	3.5 kW
Cooling power of glycol air handler	3.5 kW
PV power supplied	1.092 kW
Grid Power supplied	1.092 kW
Mass flow of the refrigerant	62.79 kg/hour
glycol pump power	35 W
glycol air handler power	200 W
HVAC air handler power	0 W*
condenser fan power	0 W*

Along with the outlined conventions in Tables 5.6 and 5.7, it was assumed that the PV modules would power the system for 7 hours out of the day, and the thermal storage would be discharging for 4 hours of the day (5-9pm).

As discussed in chapter 3, there are three modes of operation; 1) compressor cycling refrigerant to the conventional air handler, 2) compressor cycling refrigerant to the thermal storage, 3) thermal storage

discharging through the glycol air handler. Along with these three modes of operation, the HACS can be either powered from the grid or the PV modules. When the system is powered from the grid and the compressor is cycling refrigerant to either the conventional air handler or the thermal storage, the coefficient of performance can be represented by equation 2. Equation 2 can also be used to calculate the COP of the system when the thermal storage is discharging and being run from the grid. When the system is being powered by the PV modules, the power input to the system is essentially free. It is important to note that equation 2 does not take this into account. In order to calculate the COP when the PV modules are running the system, the nameplate power consumption of each running device is added up in order to figure out the power supplied. In order to find the COP of the HACS system as a whole, equation 2 is plugged into equation 3, which integrates over time allowing for a time averaged COP to be calculated.

With the previously discussed assumptions, the COP of the original prototype can be calculated and compared to the COP of conventional HVAC units. Also the COP of the second prototype AC powered system can be estimated to get a good understanding of its projected operating efficiencies. For calculating the COP of the AC powered system, the inverters efficiency (91.5%) was included in the calculation [31]. The

calculated COP's for both the original HACS prototype and the AC powered system are shown in Table 5.8.

Table 5.8 Calculated coefficients of performance

System	**COP**
HACS DC Powered	5.01
HACS AC Powered	5.03
MASTERFLUX SIERRA05-0982Y3	3.31
Ramsond AC Compressor	3.20

Table 5.8 illustrates that the AC powered system has the highest COP. This may be due to the fact that the system requires slightly less energy compared to the DC powered system. Also it is important to note that the original COP of the MASTERFLUX DC compressor that was used for the first prototype system was 3.31. It is also important to compare the separate time independent COP's of when the HACS is running in its different modes of operation. Table 5.9 through 5.10 shows the calculated COP's during the different modes of operation for both the DC and AC powered systems.

Table 5.9 Breakdown of COP for the DC powered HACS

Power Supply	Conventional HVAC Loop	Charging the Thermal Storage	Discharging Thermal Storage
Grid Power	3.043	3.043	14.89
PV Power	3.043	3.043	14.89

Table 5.10 Breakdown of COP for AC powered HACS

Power Supply	Conventional HVAC Loop	Charging the Thermal Storage	Discharging Thermal Storage
Grid Power	3.205	3.205	14.89
PV Power	2.954	2.954	13.72

Looking at table 5.9, the COP of the DC powered system when the HACS is being powered by the grid or PV modules is identical. This can be explained by the previous assumptions listed for calculating the COP. Lack of data collected with the system running plays a major role in the assumptions used to calculate the COP. When further testing is done, the COP differences between running the system from the grid or PV modules can be further differentiated. For the AC powered system, there is a greater difference between the COP of the grid powering the system and the PV modules powering the system. This can be explained due to the losses through the inverter when the PV modules are powering the system. It is also important to note the extremely high COP when the thermal storage is discharging. This is due to the fact that the glycol pump and air handler require minute amounts of power compared to running the compressor while providing similar cooling loads. Lastly, the higher COP's as displayed in table 5.8 of both the DC and AC powered systems strongly suggests that the HACS design could outperform conventional HVAC units.

5:4 POWER SAVINGS

The main reason for the creation of the HACS is to save energy. In order to fully understand the capabilities of the HACS, it is necessary to perform an analysis of the projected energy savings. As discussed in the previous sections, the PV panels could be assumed to run the system from 10am to 5pm daily for the months of May through August. The costs per kWh of electricity Arizona Power Supply's (APS) super peak energy is outlined in Table 5.11 [5].

Table 5.11 APS super peak energy plan [5]

Rate	**$/kWh**	**Time**
Off Peak	$ 0.05252	12am-12pm, 7pm-12am
Peak	$ 0.24445	12pm-3pm, 6-7pm
Super Peak	$ 0.49445	3pm-6pm

Using the outlined energy plan in Table 5.11, one can calculate the comparative costs to run the HACS system vs. a conventional HVAC unit with no PV modules. Table 5.12 shows the projected cost to run the DC and AC powered HACS system, compared with their respective systems with no thermal storage or PV modules during the months of May through August.

Table 5.12 Projected savings

System	Daily Cost $	Cost from May-August ($)
HACS DC Powered	$ 0.87	$ 106.72
Conventional DC Powered	$ 3.35	$ 411.96
HACS AC Powered	$ 0.83	$ 101.84
Conventional AC Powered	$ 3.18	$ 391.18

As is evident in Table 5.12, adding thermal storage and PV modules greatly reduces the operating costs of the system. Even though the initial costs for systems with thermal storage and PV modules are greater, the added performance benefits and cost savings in the long run are substantial.

Chapter 6: CONCLUSIONS AND RECOMMENDATIONS

This research has the potential to contribute to numerous fields of study. When the prototype system was first a plan on paper, its purpose was to lower energy usage in forward operating bases, and reduce electric costs in residential homes. Not only does the conceived prototype successfully show the potential of addressing both needs, but it also gives an indication of the potential to resolve many more problems. The installed data collection devices and constructed data compiling programs provide an excellent method of data collection and analysis. The coefficient of performance equation that has been conceived provides a solid basis with which hybrid air conditioning systems can be compared to conventional HVAC units. It is also important to note that the HACS successfully showed the ability to store energy for later use.

Both the DC or AC current systems contain multiple advantages. The DC system allows for off-grid applications; the excess PV power can be used to heat water for showers or to charge batteries for vehicles. An AC current system offers the ease of grid connection, and greater economic viability. This system as a whole has the ability to move the whole energy sector to operate at higher efficiencies, through the methods of smoothing out power generation and expenditure.

When the second prototype HACS system is completed, further data can be collected to confirm it capabilities. The second HACS will be

an updated system that will include improvements on the structural and electrical aspects. A complete analysis of the systems performance, efficiency, and benefits can be performed.

Chapter 7: FUTURE WORK

In order to fully appreciate the proposed system, testing needs to be completed for the duration of one calendar year. More temperature sensors should be installed within the thermal storage in order to gain an even better understanding of the thermal properties within the freezer. Also, temperature sensors should be placed at the fan inlet and exit of each air handler in order to collect data on the air temperatures being across the air handlers. The HACS is a heat pump, thus it can run in forward (cooling) and reverse (heating). A comprehensive thermodynamic model and analysis, along with data collection would allow for a complete understanding of the advantages of the system. From the knowledge gathered from constructing the original DC HACS system and building the second AC powered prototype, a panel should be convened to further analyze how to package the system more efficiently. After testing and data analysis, the projected costs of running the system should be compared to actual runtime costs for further insight to the economic advantages of the system. Finally, a team should be created to form a company in order optimize the packaging of the system and start production on a large-scale basis.

REFERENCES

[1] Cryogel, "Ice Ball Thermal Storage." San Diego California, June 2012, Web. <cryogel.com>

[2] Petrecca Giovanni, *Industrial Energy Management* "Principles and Applications." Norwell, MA: Kluwer Academic Publishers, 1993.

[3] "The Engineering Toolbox," May, 2012 Web. <http://www.engineeringtoolbox.com/heat-condenser-evaporator-d_881.html>.

[4] "Program announcement for FY 2013 Environmental Security Technology Certification Program (ESTCP) Installation Energy" BAA February 2, 2012, U.S. Army Corps of Engineers, Humphreys Engineer Center Support Activity.

[5] Jubran, Sadiq. *Modeling and Optimization of Hybrid Solar PV-Powered Air Conditioning System with Ice Storage*, Arizona State University, December 2011.

[6] Balmer, T. Robert, *Modern Thermodynamics,* Burlington, MA: Elsevier Inc. 2011.

[7] "Vapor-compression refrigeration." *Wikipedia.* 13 May, 2012 Web. <http://en.wikipedia.org/wiki/Vapor-compression_refrigeration>.

[8] D.S. Kim, C.A. Ferreira Infante, *Solar refrigeration options – a state-of-the-art review,* Burlington, MA. Elsevier Inc. August 6, 2007.

[9] Otanicar, Todd. "Prospects for Solar Cooling - an Economic and Environmental Assessment." *Solar Energy*86.5 (2012): 1287. Print.

[10] Global Institute of Sustainability [GIOS]. *Sustainability Initiatives Tour: Self-Guided Tour of the Tempe Campus.*2011. Arizona State University.

[11] Ice Energy, "Ice Bear Energy Storage." May, 2012 Web. <http://www.ice-energy.com/ice-bear-energy-storage-system>.

[12] Ice Bear "Product Sheet." May, 2012 Web. <http://www.iceenergy.com/stuff/contentmgr/files/1/b5fef8f4e945bef09e48aca6714b5c51/download/ice_bear_product_sheet.pdf>.

[13] Denis Du Bois. "Ice Energy's Ice Bear Keeps Off-Peak Kilowatts in Cold Storage to Reduce HVAC's Peak Power Costs." Energy Priorities Magazine, January, 16 2007 <http://energypriorities.com/entries/2007/01/ice_energy_peak_power.php>.

[14] Luftig T. Jeffrey, Jordan S. Victoria, *Design of Experiments in Quality Engineering,* New York. McGraw-Hill, 1998.

[15] H.E. Burroughs, Shirley J. Hansen, *Managing Indoor Air Quality*, Lilburn, GA: The Fairmont Press, Inc. Sep 1, 2004.

[16] "Citi-Data," May, 2012 Web. <http://www.city-data.com/forum/phoenix-area/1092335-what-do-you-set-your-c-4.html>.

[17] EVAPCO *Total Heat Versus Sensible Heat Evaporator Selection Methods and Applications,* Taneytown Maryland, EVAPCO, Inc. 2009.

[18] Beckwith Thomas G., Marangoni Roy D., Lienhard John H., *Mechanical Measurements,* 5th edition. Massachusetts: Addison-Wesley Publishing Company, 1995.

[19] Setra Sensing Solutions, "Model 209 Pressure Transducer Specifications" May, 2012 Web, <http://www.setra.com/ProductDetails/209_HVAC.htm>.

[20] Instrumart.com "King 7200 Series Specifications" May 2012 Web, <http://www.instrumart.com/products/18082/king-instrument-7200-series-rotameter>.

[21] Cen-Tech "Seven function digital multimeter; Set up and operating instructions," May, 2012 Web, <http://www.imarksweb.net/aws/view.php?u=aHR0cDovL3d3dy5o

YXJib3JmcmVpZ2h0LmNvbS9tYW51YWxzLzk4MDAwLTk4OTk5Lzk4MDI1LnBkZg==>.

[22] National Instruments *SCB-100 user Manual.* National Instruments Corporation April, 2007 <http://www.ni.com/pdf/manuals/371224b.pdf>.

[23] wunderground.com June, 2012 Web, <http://www.wunderground.com/history/airport/KPHX/2012/3/15/DailyHistory.html?req_city=Tempe&req_state=AZ&req_statename=Arizona>

[24] Duffie A. John, Beckman A. William, *Solar Engineering of Thermal Processes.* 3rd ed. Hoboken New Jersey, Jonh Wiley & Songs, Inc. 2006.

[25] Giancoli G. Douglas, *Physics: Principles with Applications,* Sixth Edition. Saddle River New Jersey, Prentice Hall. 2005.

[26] Masterflux, "SIERRA05-0982Y3, Brushless DC Variable Speed Compressor Technical Data Sheet," June 2012, Web, <masterflux.com>

[27] Google.com "100 Watt PV Module," May 2012, Web, <http://www.google.com/search?sugexp=chrome,mod=5&sourceid=chrome&ie=UTF-8&q=solar+module#hl=en&tbm=shop&sclient=psy-ab&q=solar+module+100+watt&oq=solar+module+100+watt&gs_l=serp.3...14565.14702.4.15437.2.2.0.0.0.0.110.210.0j2.2.0...0.0.UGNRBWaXiGo&pbx=1&bav=on.2,or.r_gc.r_pw.r_qf.,cf.osb&fp=5dcb926e972a056d&biw=1280&bih=685>

[28] Google Products, "LG HVAC System." May, 2012 Web. <http://www.google.com/products/catalog?q=1+ton+HVAC+air+handler&hl=en&bav=on.2,or.r_gc.r_pw.r_qf.,cf.osb&biw=1280&bih=685&um=1&ie=UTF-8&tbm=shop&cid=18216938985469124 82&sa=X&ei=peSNT47YLcHe2QWr1PmODA&ved=0CFAQ8gIwAA>.

[29] Vetco Electronics, "Cables Connectors and More." May, 2012 Web. <http://shop.vetcosurplus.com/catalog/product_info.php?products_id=7787>.

[30] Ramsond Sensible Solutions June, 2012 Web,<http://ramsond.com/>

[31] SMA Solar Technology. May, 2012 Web. <http://www.sma-america.com/en_US.html>.

[32] Comfort.com, May, 2012 Web. <http://ecomfort.com/products/mitsubishi-mszfe09namuzfe09na-mr-slim-wall-mounted-single-zone-heat-pump-9000btu/3363>.

[33] Bell, Arthur A. *HVAC equations, data, and rules of thumb*. 2nd ed. The Mcgraw-Hill Companies, 2008.

APPENDIX A

TEST PROCEDURES

Experiment 1: List of Variables

Independent Variables	Dependent Variables	Constant Variables	Non-Manipulated Variables	Calculations
Room Temperature / load	Energy used to charge the thermal storage	DC compressor RPM	Outside temperature	Cooling power of HVAC air handler
	Energy required to run the system	Glycol flow rate	Solar radiation	Cooling power of glycol air handler
	How long TS lasts before complete discharge	Fan speed of glycol air handler		Cost of grid power / Energy savings
	Max cooling power			COP of system
				Load on HACS vs. Room temperature
				PV power consumed vs. supplied

Experiment 1 procedure

A. Day 1
    1. Turn on system
        i. Turn on system at 7pm
    2. Set thermostats
        i. Low thermostat (HVAC air handler)
            a. Set to 72 degrees
        ii. High thermostat (Glycol air handler)
            a. Set to 73 degrees
    3. Running schedule
        i. 7pm-7am
            a. Let system run off the grid, meeting the room temperature requirements and charging the thermal storage when HVAC unit is not running.

ii. 7am-12pm
    a. Observe amount of ice storage accumulated at 7am (record this)
    b. Let the system run off combined grid/PV power
    c. Observe amount of ice storage accumulated by 12pm (record this)
iii. 12pm-7pm
    a. Let system run off of PV power as long as possible.
    b. Once there is insufficient PV power, turn off HVAC air handler side, and run only the glycol thermal storage system
        - Take note of how much ice had built up at this point
    c. Set the high thermostat to 73 degrees
        - Note – if not enough ice has built up let conventional HVAC side stay on for these hours and be powered by PV/grid

B. Day 2
1. Running schedule
i. 7pm-7am
    a. Set low thermostat to 72 degrees
    b. Set high thermostat to 73 degrees
    c. Let system run off of grid power over night to meet room temp demands and charge the thermal storage
        - Note ice storage volume at 7pm
ii. 7am-12pm
    a. Let system run off of PV/grid power
    b. Keep both thermostats at the same setting
        - Note ice storage volume at 7am and 12pm

iii. 12pm-7pm
    a. Run system off the PV power only until insufficient PV power is supplied
    b. Once there is not enough PV power, turn off the HVAC side and compressor. Only use the glycol thermal storage
        - Note ice storage at moment when HVAC/compressor is turned off.
        - Record the ice storage volume at 7pm

C. Day 3
    1. Run schedule
        i. 7pm-7am
            a. Set low thermostat to 72 degrees
            b. Set high thermostat to 73 degrees
            c. Let system run off of grid power over night to meet room temp demands and charge the thermal storage
                - Record the ice storage volume 7am
        ii. 7am-12pm
            a. Let system run off of PV/grid power
            b. Keep both thermostats at the same setting
                - Record the ice storage volume at 12pm
        iii. 12pm-7pm
            a. Run system off the PV power only until insufficient PV power is supplied
            b. Once there is not enough PV power, turn off the HVAC side and compressor. Only use the glycol thermal storage
                - Record the ice storage volume

D. Day 4
    1. Run schedule
        i. 7pm-unknown
            a. Discharge the thermal storage fully
                - Observe how long the TS lasts (time)
                - Note when cooling power gets below 1 ton

E. Repeat (A-D) with setting the two thermostats within a range of (66-80^{o}F) in 2^{o} increments.

Experiment 2: Variables

Independent Variables	Dependent Variables	Constant Variables	Non-Manipulated Variables	Calculations
Glycol flow rate	Energy used to charge the thermal storage	DC compressor RPM	Outside temperature	Cooling power of HVAC air handler
	Energy required to run the system	Room temperature / load	Solar radiation	Cooling power of glycol air handler
	How long TS lasts before complete discharge	Fan speed of glycol air handler		Cost of grid power / Energy savings
	Max cooling power			COP of system
				Load on HACS vs. Room temperature
				PV power consumed vs. supplied

Experiment 3: Variables

Independent Variables	Dependent Variables	Constant Variables	Non-Manipulated Variables	Calculations
DC compressor RPM	Energy used to charge the thermal storage	Glycol flow rate	Outside temperature	Cooling power of HVAC air handler
	Energy required to run the system	Room temperature / load	Solar radiation	Cooling power of glycol air handler
	How long TS lasts before complete discharge	Fan speed of glycol air handler		Cost of grid power / Energy savings
	Max cooling power			COP of system
				Load on HACS vs. Room temperature
				PV power consumed vs. supplied

Experiment 4: Variables

Independent Variables	Dependent Variables	Constant Variables	Non-Manipulated Variables	Calculations
Fan speed of glycol air handler	Energy used to charge the thermal storage	DC compressor RPM	Outside temperature	Cooling power of HVAC air handler
	Energy required to run the system	Room temperature / load	Solar radiation	Cooling power of glycol air handler
	How long TS lasts before complete discharge	Glycol flow rate		Cost of grid power / Energy savings
	Max cooling power			COP of system
				Load on HACS vs. Room temperature
				PV power consumed vs. supplied